Available online at https://link.springer.com/journal/42241
http://www.jhydrodynamics.com
Journal of Hydrodynamics, 2021, 33(3): 400-420
https://doi.org/10.1007/s42241-021-0043-7

Flow dynamics and sediment transport in vegetated rivers: A review *

Wen-xin Huai[1], Shuolin Li[2, 3], Gabriel G. Katul[2, 3], Meng-yang Liu[1], Zhong-hua Yang[1]
1. *State Key Laboratory of Water Resources and Hydropower Engineering Science, Wuhan University, Wuhan 430072, China*
2. *Department of Civil and Environmental Engineering, Duke University, Durham, NC, USA*
3. *Nicholas School of the Environment and Earth Science, Duke University, Durham, NC, USA*

(Received March 10, 2021, Revised May 10, 2021, Accepted May 11, 2021, Published online June 23, 2021)
©China Ship Scientific Research Center 2021

Abstract: The significance of riparian vegetation on river flow and material transport is not in dispute. Conveyance laws, sediment erosion and deposition, and element cycling must all be adjusted from their canonical rough-wall boundary layer to accommodate the presence of aquatic plants. In turn, the growth and colonization of riparian vegetation are affected by fluvial processes and river morphology on longer time scales. These interactions and feedbacks at multiple time scales are now drawing significant attention within the research community given their relevance to river restoration. For this reason, a review summarizing methods, general laws, qualitative cognition, and quantitative models regarding the interplay between aquatic plants, flow dynamics, and sediment transport in vegetated rivers is in order. Shortcomings, pitfalls, knowledge gaps, and daunting challenges to the current state of knowledge are also covered. As a multidisciplinary research topic, a future research agenda and opportunities pertinent to river management and enhancement of ecosystem services are also highlighted.

Key words: Canopy flow, river morphology, riparian vegetation, sediment transport

Introduction

Rivers and streams are rightly labeled as the "veins" of the hydrological cycle as they offer an efficient passage of material and energy, and they carry substantial biogeochemical information on land-use legacies. After all, the fastest velocities associated with hydrological processes are those of flowing water in rivers and streams, at least when compared to subsurface flow, interflow, overland flow, evapotranspiration, or water flow within plants. The terms river and stream are used interchangeably here though rivers tend to be longer, larger, and deeper than streams. Aquatic vegetation is vital to the maintenance and restoration of rivers. Vegetation affects the flow dynamics and sediment movement in rivers, and thus affects their physical and ecological function[1], which is the compass of this review. The presence of vegetation is conducive to slowing down river erosion and stabilizing floodplain or riverbanks. Aquatic plants not only directly absorb pollutants such as nitrogen and phosphorus, but also promote oxidation and decomposition of pollutants and improve the self-purification ability of rivers by changing their micro-environment. Vegetation also provides a suitable habitat for aquatic animals that contribute to the development of aquatic species diversity. The sediment particles in water adsorb heavy metals, nitrogen, phosphorus and other nutrients, thus acting as the main carrier and medium of material migration and transformation.

On short time scales, the presence of vegetation increases flow resistance, changes the transverse and vertical flow structure (measured by sizes of coherent structures), and affects the balance of sediment suspension and deposition. The sediment transport capacity is also diminished in the so-called "vegetation region" as the bed shear stress is reduced through momentum absorption by aquatic plants. On longer time scales, the dynamics of vegetation biomass within rivers is closely related to sediment deposition and erosion, which can impact organic materials that then promote vegetation patch extension within the river[2]. Such feedbacks between vegetation growth and sediment deposition and erosion are likely

* Projects supported by the National Natural Science Foundation of China (Grant Nos. 52020105006, 11872285), the U.S. National Science Foundation (Grant Nos. NSF-AGS-1644382, NSF-AGS-2028633 and NSF-IOS-1754893).
Biography: Wen-xin Huai (1963-), Male, Ph. D., Professor, E-mail: wxhuai@whu.edu.cn
Corresponding author: Zhong-hua Yang, E-mail: yzh@whu.edu.cn

to remain the subject of active research and future development[3-5], which will be partially covered in this review.

River morphodynamics investigates natural patterns observed in the sedimentary environments of river ecosystems, which invariably arise from the mechanical interaction between sediments and the flow[6]. As an active part of the river ecosystems, the presence of aquatic vegetation significantly affects river morphology operationally divided into three types: braided, meandering and straight[7]. In turn, the colonization and growth of aquatic vegetation requires water, sediments, nutrients and seeds to be transported within rivers[8].

The interaction between vegetation, flow and sediment draws on a number of traditional and emerging fields including turbulence, ecological hydraulics, sediment transport, hydro-geomorphology among others. With advancements in theory, experiments, and simulations, the scope of geomorphology and river reaches has gradually developed to consider local scale and plant scales[9] in ways not possible few decades ago. With such fine-scaled processes directly considered, the interplay between water conveyance laws and material migration laws has been obtained in the presence of vegetation. The purpose of this review is to feature research progress related to the role of vegetation on flow dynamics and sediment movement, highlight current research opportunities and challenges, and put forward the corresponding prospects for the problems to be solved.

1. Hydrodynamics of vegetated channels

1.1 *Definitions and review of key concepts in open channel flow*

It is convenient to commence the discussion with a simplified setup comprising a rectangular open channel with a constant slope S, channel width W, and length L. The flow is assumed to be steady and uniform with a constant flow rate Q and water depth H (Fig. 1). In the absence of any plants, the continuity (or conservation of water mass) equation leads to a bulk velocity defined as $U_b = Q/(WH)$. The shear stresses arising from water movement are assumed to be uniformly distributed and acting along the channel sides and bed (τ_o). Along the direction of the flow (designated by x), uniform flow requires a balance between the gravitational forces driving movement and frictional stresses resisting its motion. For small slope angles, this force balance leads to $u_*^2 = \tau_o/\rho = gR_hS$, where g is the gravitational acceleration, $R_h = H(1+2H/W)^{-1}$ is the hydraulic radius, ρ is the water density (assumed constant throughout), and u_* is the friction or shear velocity. Additionally, for wide channels ($H/W \ll 1$ and thus $R_h/H \approx 1$), the shear stress distribution $\tau(z)$ must decrease linearly from a maximum τ_o to its value at the free water surface, which is assumed to be zero when neglecting any air-water interactions. Hence, $\tau(z)/\tau_o = 1 - z/H$, where z is the normal distance from the channel bed.

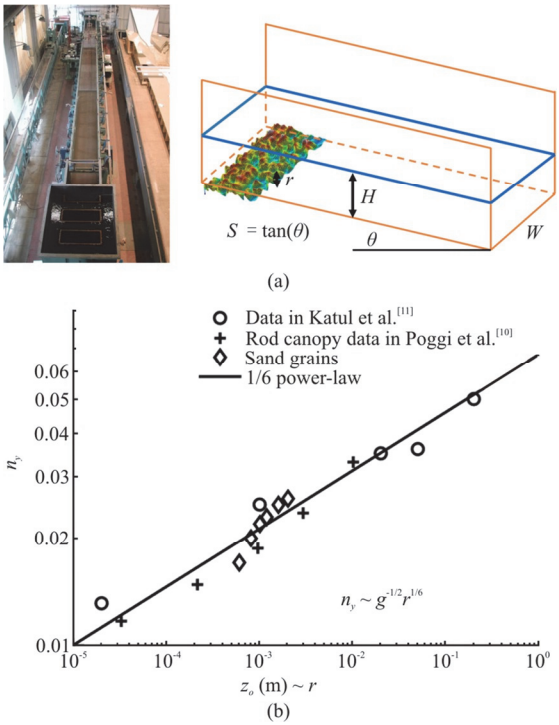

Fig. 1 (Color online) (a) Representation of idealized open channel flow in a rectangular channel, where r is the mean protrusion height. (b) Relation between Manning roughness ($n_y \sim g^{-1/2} r^{1/6}$) and the momentum roughness height z_o assumed to scale with the mean protrusion height. The data include sand grains, random roughness elements[10-11], and submerged rods where the rod height is much smaller than the water depth

The main water conveyance equation, the so-called Chezy-equation, arises when linking u_*^2 to U_b^2 using a bulk drag coefficient $C_{d,b} = u_*^2/U_b^2$ resulting in $U_b = (C_{d,b})^{-1/2}\sqrt{gR_hS}$. Much of the early research in hydraulics was focused on linking $C_{d,b}$ (or a related property – the Darcy-Weisbach friction factor) to R_h, the geometric properties of the roughness elements distributed along the bed and channel sides (e.g., r), and the bulk Reynolds

number $Re_b = U_b R_h / \nu$, where ν is the kinematic viscosity. It was found that when $Re_b > 500$ (high Reynolds number), $C_{d,b} \sim (r / R_h)^{1/3}$ and is no longer impacted by Re_b (the so called Strickler scaling), where r is the mean protrusion height of the roughness elements provided $r / Re_h \ll 1$. Throughout, the symbol "~" implies scale as. For $C_{d,b} \sim (r / Re_h)^{1/3}$, the $U_b \sim R_h^{2/3}\sqrt{S}$, which is the well-known Manning formula. Its associated Manning roughness $n_y \sim g^{-1/2} r^{1/6}$ thereby establishing a direct link between roughness protrusion r and resistance to flow. The $n_y \sim r^{1/6}$ has received broad experimental support but a number of issues remain to be resolved regarding the range of applicability and its theoretical justification[12-13]. Likewise, when $Re_b < 10$, $C_{d,b} \sim 1 / Re_b$ resulting in $U_b \sim \nu^{-1} R_h^2 g S$, which is analogous to Darcy's law upon noting that $S = -\mathrm{d}H / \mathrm{d}x$ in uniform flow, U_b is a flux of water, and $g\nu^{-1}R_h^2$ is a hydraulic conductivity. More broadly, the conveyance laws for open channel flow in the absence of vegetation can be summarized by a single relation of the form $Fr^2 = U_b / (gR_h S) = (C_{d,b})^{-1} = f(Re_b, r / R_h)$, where Fr is a Froude number and $f(\cdot)$ signifies a function of (in this case two dimensionless quantities–bulk Reynolds number and relative roughness) as discussed elsewhere[12, 14]. Non-rectangular cross-sections lead to different $f(\cdot)$ but the two key dimensionless quantities remain unaltered. For this reason, the primary focus here is on rectangular sections.

From the flow energetics perspective, the work needed per unit mass per unit time to move clear water at a rate Q is gSU_b. In steady-uniform flow, this work is supplied by the gravitational force but dissipated (or converted to heat) by frictional forces allowing an estimate of the bulk dissipation rate as $\varepsilon_b = gSU_b = (u_*^2 / R_h) u_* (C_{d,b})^{-1/2}$ or alternatively $\varepsilon_b = C_{d,b}(U_b^3 / R_h)$. This normalized $R_h \varepsilon_b / U_b^3 = C_{d,b}$ has received experimental support and establishes link between $C_{d,b}$ and maximum entropy production principles[15].

We now ask how the presence of aquatic plants alter these key results? Are plants simply acting as tall roughness elements (i.e., r / R_h is no longer $\ll 1$)? Given that plants exert an additional drag force, can this drag force be represented as an equivalent bed or side shear stress (i.e., simply increasing τ_o or r under some conditions (e.g., for submerged plants where H is much larger than the canopy height as suggested by Fig. 1)? How is the linearity in the stress distribution (i.e., $\tau(z) / \tau_o = 1 - z / H$) altered by the presence of aquatic vegetation and what are its consequences on a plethora of applications such as sediment transport? How are the energetics of the flow, including ε_b, altered by the presence of stems due to wake generation and other vortical motion?

1.2 *Aquatic vegetation and its representation*

Aquatic plants are divided into three types: emergent, submerged, and floating vegetation. Defining the plant height as h, the submergence parameter H / h dictates whether plants are emergent (i.e., $H / h < 1$), submerged or floating $(H / h > 1)$. Aquatic plants can be further divided into rigid and flexible based on whether they have obvious bending deformation when subjected to water flow. Flexible vegetation does have the capacity to reduce local drag forces by deformation (bending or waving) though the current review is primarily focused on rigid vegetation. Given the complex geometry of real plants, the representation of aquatic vegetation is usually simplified to a rigid circular cylinder array with uniform diameter, which is a reasonable generalization for plants with fewer branches and leaves below the water surface[1, 16-18]. The distribution characteristics of vegetation can be parameterized by the number of stem roots per unit bed area. Assuming that the mean diameter of plant stem is d and the number of stems per unit bed area is n, the vegetation density can be characterized by the solid volume fraction occupied by the vegetation elements and given as

$$\lambda = \frac{n\pi d^2}{4} \tag{1}$$

For the purposes of drag force representation, it is more convenient to use the projected frontal area orthogonal to the flow per vegetation volume and is given by

$$a = nd \tag{2}$$

For submerged and floating vegetation, it is usually more reasonable to utilize the dimensionless parameter ah to characterize the vegetation density, which represents the frontal area per bed area and is known as the roughness density[19].

1.3 *Flow resistance*

Compared with an open channel characterized by a bare bed, the presence of aquatic vegetation induces significant flow resistance, which slows down the

flow and raises the water level, thus reducing the flood carrying capacity of a river. Undoubtedly, vegetation drag is a necessary factor for describing the hydrodynamics of vegetated channels. The vegetation resistance is linked to the drag force usually parameterized by a quadratic drag law and is given as

$$F_d = \frac{1}{2} C_d \rho d h U_p^2 \tag{3}$$

where ρ is the density of water, C_d is a local drag coefficient (that differs from $C_{d,b}$) to be discussed, U_p is the double averaged (time-averaged and space-averaged) "pore velocity" within the vegetation area and is given by $U_p = Q/[WH(1-\lambda)]$.

The plant drag coefficient, C_d, varies with the flow conditions and vegetation distribution. In analogy to $C_{d,b}$, a stem Reynolds number is needed and is defined as $Re_p = U_p d/\nu$. For an isolated cylinder, the C_d, first decreases with the increases in Re_p. With further increases in Re_p, the C_d remains roughly constant independent of Re_p except at very high Re_p. At such very high Re_p, C_d drops suddenly and then gradually recovers via a phenomenon known as the "drag crisis"[20]. A similar dependency has also been observed for the vegetation drag coefficient[21-23]. When Re_p is relatively low, C_d decreases sharply with increases in Re_p, while C_d remains of order unity when $Re_p > 300$. At the same time, C_d also increases with vegetation density, due to the accompanying decreased flow area and enhanced stem-wake and wake-wake interaction[10]. Based on experiments and numerical calculations and with the help of various data-driven methods, a large number of C_d prediction models have been established, which were reviewed by D' Ippolito et al.[24] and Liu et al.[22]. In addition to the Reynolds number and vegetation density, the distribution pattern of vegetation elements also affect the drag force[25-26]. Generally, the C_d value of square configuration appears to be smaller than that of random and staggered configuration. When vegetation elements are square arranged, the downstream stems are directly located in the wake of the upstream stems, causing the downstream stems to suffer a lower approach velocity and thus low stagnation pressure. Also, the turbulence provided by the wake of upstream stem could delay the boundary layer separation of the downstream one, thus resulting in a low pressure difference between the frontal and rear surfaces of the downstream stem[23].

At the "reach" scale, the flow resistance induced by aquatic vegetation is determined by the ratios of average height (h) of vegetation community to H and average width (w) of vegetation community to channel width (W)[27-29], and it can be parameterized by a blockage ratio $\psi = wh/(WH)$. At this scale, the geometry of plant stems is not significant and flow resistance is usually expressed by a Manning roughness n_v. Thus, for emergent vegetation, the n_v increases with flow depth H whereas for submerged vegetation, n_v decreases nonlinearly with increases in submergence H/h [30-31]. In rough-wall turbulent open channel flow without vegetation, $n_y \sim r^{1/6}$ and does not dependent on H that is presumed to be much larger than r[11]. To summarize, Table 1 shows how the presence of rigid vegetation alters (or adds) key variables to the conveyance laws for water movement depending on the submergence ratio.

1.4 *Flow in emergent vegetation*

Emergent vegetation refers to aquatic plants that fill the entire flow depth and even penetrates above the water surface. The existence of vegetation elements breaks large-scale vortices into small-scale vortices, especially those larger than the stem diameter, d, and the space between vegetation elements, s. When $Re_p > 120$, the stem wake becomes turbulent and the stem vortex at the scale of d is generated[41]. This stem wake provides additional turbulent kinetic energy. When vegetation

Table 1 Summary of key models for flow resistance

Open channel flows	Conveyance law	Key parameters
Without vegetation	$Fr = f\left(\frac{r}{R}, Re_b\right)$ [32-34]	$\frac{r}{R}$, Re_b
With emergent vegetation	$Fr = f(C_{d,b}, Re_p)$ [21,-22, 35-36]	$C_{d,b}$, Re_p
With submerged vegetation	$Fr = f\left(\frac{\lambda\delta_e}{H-h_v}, C_{d,b}, \frac{h_v}{H}\right)$ [37-40]	λ, δ_e, $C_{d,b}$, $\frac{h_v}{H}$

density is very high, $d > s$, the dominant turbulence length scale is s, however, when vegetation is sparse, $d < s$, the dominant turbulence length scale is d. That is to say, in vegetated flow, the turbulence length scale that is most restrictive is $l = \min(d, s)$, rather than H [42] in the absence of vegetation. Even in very sparse vegetation, the turbulence generated by stem wakes is at least equivalent to that produced by bed shear. Consequently, in vegetated flow, the turbulent kinetic energy and its dissipation rate cannot be estimated from bed shear stress but should depend on vegetation resistance. Recall that $\varepsilon_b = (u_*^2 / R_h) u_* (C_{d,b})^{-1/2}$ and thus is entirely driven by surface shear stress or $u_* = \sqrt{\tau_o / \rho}$ in non-vegetated open channel flow. The generation of stem scale vortices transfers energy from the mean flow to the turbulence, which is mainly achieved by the work done by the flow overcoming vegetation resistance[43]. Regardless of energy loss, the turbulent kinetic energy (TKE) in vegetation can be related to $C_d a l$ and increases with increasing λ [42]. However, when the driving force is fixed, there is a non-monotonic relation between TKE and vegetation density[23]. Specifically, the turbulent kinetic energy increases with λ when vegetation is relatively sparse; however, it decreases with the increasing λ when vegetation density reaches a certain value. This non-monotonic behavior was confirmed in numerical studies[44].

As mentioned above, due to the presence of stem elements, the flow in vegetated region becomes spatially heterogeneous at the stem scale. Therefore, it is necessary to average such variability out when deriving conveyance laws. To remove such spatial heterogeneity[43], the double averaging method is used. This method introduces a spatial averaging operator over stem scales above and beyond the common temporal averaging. The Cartesian coordinates x and y are defined as streamwise and lateral direction, respectively, while z is normal to the bed surface as before. Correspondingly, the instantaneous velocity components in three directions are u, v and w, respectively. Applying the double averaging method to the streamwise momentum equation and considering steady uniform flow yields

$$gS - \frac{1}{\rho}\frac{\partial \langle \overline{p} \rangle}{\partial x} + \nu \frac{\partial^2 \langle \overline{u} \rangle}{\partial z^2} - \frac{\partial \langle \overline{u'w'} \rangle}{\partial z} - \frac{\partial (\overline{u}''\overline{w}'')}{\partial z} - \frac{1}{2}\frac{C_d a}{1-\lambda} \langle \overline{u} \rangle \left| \langle \overline{u} \rangle \right| = 0 \quad (4)$$

where p is the instantaneous pressure, overbar and angle bracket represent time and spatial averages, respectively; the single and double prime represent the deviations from the time average and the spatial average, respectively. On the right hand side of Eq. (4), the first term is the streamwise component of gravity, the second term is the mean pressure gradient, which can be approximated from hydrostatic conditions, $\partial \langle \overline{p} \rangle / \partial x = \rho g \partial H / \partial x = 0$ in uniform flow, the third term is the viscous stress, which can be ignored compared with the vegetation resistance except for the region very close to bed surface, the fourth term is the spatial averaged Reynolds stress, and the fifth term is the dispersive stress originating from spatial averaging. Within vegetated area, since the vortex length scale is dominated by the smaller of d and s, which is far less than the flow depth H, the turbulent momentum flux is significantly limited. Also, the dispersive flux is negligible when $ah > 0.1$ [45-46]. That is, the fourth and fifth terms of Eq. (4) can be ignored yielding[47]

$$\langle \overline{u} \rangle = \sqrt{\frac{2gS(1-\lambda)}{C_d a}} \quad (5)$$

Based on Eq. (5), the flow velocity in emergent vegetation can be estimated provided C_d can be externally supplied. Furthermore, it can be seen from Eq. (5) that the double averaged velocity $\langle \overline{u} \rangle$ along the vertical direction is related to $C_d a$, that is, the larger the $C_d a$, the smaller the $\langle \overline{u} \rangle$. For the idealized emergent aquatic vegetation modeled as a rigid cylinder array, $C_d a$ is constant along the water depth, so the average velocity is also almost constant along the vertical direction[48], an assertion supported by experiments and model runs[47]. However, near the bed surface, the velocity distribution has a local maximum, which is mainly attributed to the horseshoe vortex system formed at the junction of vegetation elements and bed surface[26, 48-49].

1.5 *Flow in submerged and floating vegetation*

For submerged vegetation, due to the discontinuity of flow resistance at the vegetation interface, the velocity of the free flow region above vegetation is higher than that of the vegetation region, resulting in the generation of the vegetation shear layer at the top of the vegetation area. The vegetation shear layer is similar to the free shear layer, and the velocity distribution at the top of the vegetation region is analogous to a "mixing layer" characterized by an inflection point[50-51]. This induces flow instability and leads to the generation and development of

Kelvin-Helmholtz (K-H) vortices[50], an analogy first put forth in terrestrial vegetation turbulence studies. At the vegetation interface, the transport of momentum and mass is mainly dominated by the vegetation-scale vortices[48, 52-57], which can be visualized utilizing the Liutex vortex identification method[58-59]. Due to the presence of a vegetation shear layer, the Reynolds stress and mean velocity reach a maximum at the top of the vegetation, and gradually decrease towards the water surface and the bed, as shown in Fig. 2(a).

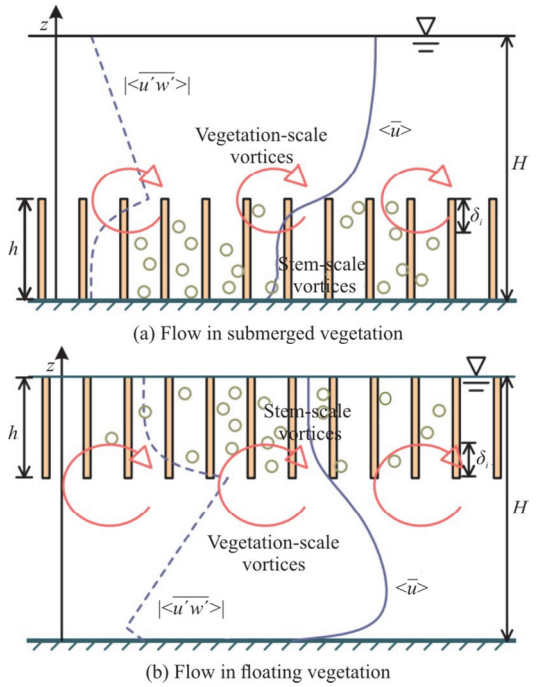

Fig. 2 (Color online) Schematic view of the flow

In the free shear layer, the K-H vortices can continuously grow downstream[60]. However, in the vegetation shear layer, subjected to vegetation resistance, the growth of K-H vortices will be arrested when reaching a certain scale, which occurs when the energy extracted by mean shear is in balance with the dissipation of vegetation resistance[52-53]. At this time, the distance of K-H vortices penetrating into vegetation area is δ_i (i.e., the inner layer of the mixing layer), which is inversely proportional to the drag parameter of vegetation[61]

$$\delta_i = \frac{0.23 \pm 0.06}{C_d a} \tag{6}$$

In experiments, this so-called "penetrating depth" δ_i is usually defined as the distance between the vegetation interface and the vertical position where Reynolds stress decreases to 10% of its maximum towards the bed[62]. In addition to vegetation resistance and vegetation density, the submergence also affects the penetrating depth. When vegetation is shallow submerged, $H/h < 2$, the development of K-H vortices will be inhibited by the free water surface (mainly by limiting the growth of its outer layer)[63-64]. As mentioned above, the K-H vortices dominate the turbulence intensity near the vegetation interface, while the turbulence level in the lower vegetation layer, $z < h - \delta_i$, is dominated by the stem-scale vortices. It should be noted that the vegetation shear layer vortices only occur when $C_d ah \geq 0.1$ [61, 65], a condition also investigated in flume studies[10]. In particular, at $0.1 \leq C_d ah \leq 0.23$, Eq. (6) shows that the K-H vortices penetrate the entire vegetation height all the way to the bed, which significantly elevate the turbulence intensity near the bed and benefits the resuspension of sediment (discussed later). However, at $C_d ah < 0.1$, that is, the vegetation resistance is less important than bed friction, the velocity distribution follows a classical logarithmic distribution of turbulent boundary layer, and the vegetation elements just behave as bed roughness but displaced by a so-called zero-plane displacement. An estimate of the zero-plane displacement height is the centroid of the drag force.

Different from emergent vegetation, the vertical distribution of longitudinal velocity of submerged vegetation exhibits obvious zonal characteristics. In the lower vegetation layer $(z < h - \delta_i)$, the flow is similar to that of emergent vegetation and mainly driven by gravity and pressure potential. In the upper vegetation layer $(h - \delta_i < z < h)$, besides the gravity and pressure potential, the Reynolds stress is also an important driving force. The overlying flow above the vegetation region is similar to the open channel flow. Based on the momentum balance and turbulence theory in each layer, various n-layers models have been developed to represent the full variation of the mean velocity distribution[66-69]. The general approaches were summarized by Nepf[70]. In these models, the drag coefficient C_d is a necessary parameter that needs to be measured or estimated in advance. Generally, $C_d = 1$ is reasonable over a large Reynolds number range $(800 < Re_p < 8\,000)$ [66]. For the estimation of the bulk velocity of the entire flow section, the Chézy formula can be used in which the Chézy coefficient of submerged vegetation depends on C_d, H/h, and λ [37-38] as reviewed elsewhere[24].

Floating vegetation refers to aquatic plants that are suspended along the free water surface, forming a floating treatment wetlands. This new artificial infrastructure was introduced in recent years for

watstewater treatment[71], which has been shown capable of enhancing the contaminants removal efficiencies[72-73]. The aquatic plants extend downward while maintaining a gap with the bed surface (Fig. 2(b)). In floating vegetation, when the vegetation density is sufficiently large so as to provide enough resistance to induce an inflection point in the mean velocity profile at the vegetation interface, the vegetation-scale vortices would form and dominate the turbulence transport between the vegetation area and the gap region below floating vegetation[74-77]. Different from the common submerged vegetation described above, the growth of the outer layer of the floating vegetation is significantly inhibited by the bed boundary layer. Meanwhile, these shear vortices enhance the turbulence near the bed. The velocity distribution also has obvious divisions, which can be generally divided into bottom boundary layer, vegetation shear layer, and upper vegetation layer, and can be modeled using various analytical approaches[78-81]. In the bottom boundary layer, turbulence is supplied by bed shear, while in the vegetation shear layer, the K-H vortices dominate the turbulent flux[1, 82]. Finally, in the upper vegetation layer, the turbulence is characterized by stem-scale vortices analogous to the emergent vegetation case.

1.6 *Flow through and around finite vegetation patches*

The contents described above are for vegetated flow in fully covered channels. However, in rivers and shallow lakes, aquatic plants often exist in patches with limited size and appear to be approximately circular[83-84]. Compared with the flow in fully vegetated channels, the flow through and around limited vegetation patches is more complicated[85-91] and has been the subject of detailed experiments recently[89]. As the incoming flow approaches the vegetation patch, the flow deflects laterally to both sides, and more importantly, a portion of the incoming flow passes through the vegetation patch, known as “bleeding flow”. After entering the patch, and due to the resistance induced by vegetation elements within the patch, part of the flow continues to deflect laterally and exits the patch, and the other part of the flow exits the patch streamwise. Downstream of the vegetation array, a steady wake region is formed in which the flow is approximately laminar and constant along the streamwise direction. At the end of the steady wake region, the longitudinal velocity gradually recovers to the incoming flow level. The lengths of the steady wake region and the recovery region decrease with the increasing vegetation density[92]. The streamwise momentum entering the steady wake region inhibits the interaction of the two shear layers formed on both sides of the patch, thus suppressing the generation of the patch-scale Karman vortex streets just as an isolated cylinder as shown in Fig. 3(a). Depending on λ, three regions were identified: (1) at $\lambda < 0.05$, the vegetation stems inside the array behave as isolated cylinders (2) at $0.05 < \lambda < 0.15$, the collective behavior of the patch appears and two shear layers are formed at the shoulders of the patch and interact with each other at the end of the steady wake region and generate wake billow vortices, and (3) at $\lambda > 0.15$, the vegetation patch behaves as a solid cylinder with the same diameter and produces a Karman vortex street at the patch scale[93].

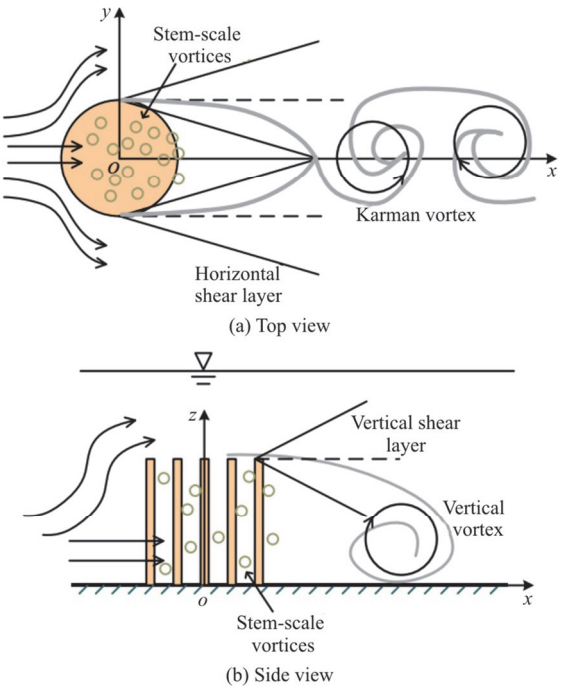

Fig. 3 (Color online) Schematic of the flow structure through and around a submerged vegetation patch

Aquatic vegetation is usually submerged during the early growth stage and flood period. Compared with an emergent patch, when the incoming flow approaches the submerged array, in addition to deflecting towards both sides, the flow is also diverted over the top of the patch, and vertical bleeding flow occurs whose strength also depends on λ [89, 94-96]. There is a strong downflow downstream of the patch, similar to a solid cylinder, which further suppresses interaction of horizontal shear layers. When the aspect ratio of the vegetation patch is greater than a certain threshold, vertical vortices will form downstream of the patch (Fig. 3(b)), which makes the wake structure of submerged vegetation patch three-dimensional[94]. Upstream of the patch, if the vegetation can produce enough adverse pressure gradient, horseshoe vortex systems will be generated at the root of the vegetation patch, which will cause significant erosion[97-98].

2. Incipient sediment motion in the vegetated flow

The estimation of incipient sediment motion in vegetated open channel flow plays a significant role in protecting riverbed from erosion and sediment transport as well as restoring ecological function. However, only a few studies have investigated the incipient sediment motion in flows with vegetation[24, 80-85].

2.1 *Effects of vegetation on the incipient sediment motion*

The incipience of sediment motion is controlled by flow conditions. When the flow intensity exceeds a certain value, sediment particles initiate motion[99]. Vegetation has a significant impact on the flow field, which affects the incipient sediment motion and makes it much more difficult to predict when compared with open channel flow over the bare river bed. To be specific, on the one hand, the additional vegetation drag reduces the mean flow and the bed shear stress within vegetated regions compared with the non-vegetated open-channel regions[23, 100, 101]. This effect dampens the motion of sediment particles, thus helping to reduce bed erosion. On the other hand, the vegetation also influences the intensity of turbulence. The introduction of sparse vegetation can augment the turbulence intensity due to the additional production of turbulence by stem wakes[23]. This indicates that vegetation can contribute positively to the incipient sediment motion. In addition, the bed shear stress and flow field become spatially heterogeneous while the flow is forced to move around each vegetated stem[27], which may lead to the incipient motion of sediment particles varying with its position and controlled by the local flow conditions[102]. Actually, previous experiments note that sediment particles around vegetated stems initiate motion as the local velocity increases[103]. Then, local scour holes are formed at the root of the stems. Subsequently, the sediment particles washed away from the scour holes are transported downstream, which leads to the formation of sand waves. The sand waves develop in size until a steady-state is reached[104-108].

2.2 *Criterion of incipient sediment motion in vegetated open channel flow*

In non-vegetated open channels, the shear stress and the critical flow velocity are usually used as the hydraulic parameters to describe incipient sediment motion[99]. Early studies of sediment transport in flow with vegetation were mainly concerned with the effect of vegetation resistance on bed shear stress. In fact, the total shear stress defined at the top of the vegetated canopy could be decomposed into a bed shear stress and a vegetation drag force[27, 109]. Thus, the bed shear stress can be obtained by subtracting the vegetation drag force from the total flow stress (a form of partition method), the latter determined from overall momentum considerations. Using this method, the bed load transport to calculate the bed shear stress in vegetated open channel flow have been proposed[110-111]. In these calculations, the critical bed shear stress of incipient sediment motion is naively regarded as the same as that in non-vegetated open channels. However, studies on bed load transport for flow with emergent vegetation found that the critical bed shear stress of incipient sediment motion was higher than that of non-vegetated open channel flow[108]. In addition, the critical bed shear stress appeared higher in flows with smaller stem diameter under similar vegetation density. Experiments that explore the incipient motion of sediment with a submerged flexible vegetation patch have already been undertaken[107]. These experiments reported that the average of the Shields parameter in the patch section is much larger than that reported for open channels without vegetation. Those studies revealed that the critical bed shear stress of incipient sediment motion under the impact of vegetation must be different from the one in non-vegetated open channel flow and it is influenced by the characteristics of vegetation. However, in much of these studies, the bed shear stress is relatively small since vegetation resistance generally accounts for the vast majority of the total flow resistance. Naturally, inferring such a small stress from the partition method can be "plagued" by large errors. Practically and pragmatically, the bed shear stress may be deemed unsuitable for a threshold condition to describe incipient sediment motion in vegetated open channel flow.

From experiments, Tang et al.[104] concluded that the status of the incipient motion of sediment in vegetated open channel flow could be classified into one of three stages. The first stage is a no sediment movement over the whole bed. In the second stage, the sediment particles around vegetation stems commence their motion and the sand waves reached an equilibrium state as mentioned above, but the velocity was not high enough to transport the sediment out of the vegetated zone. Tang et al.[104] stated that in the above stages no net bed load transport occurred. With the flow velocity continuing to increase to a certain threshold value, noticeable sediment particles begun to be transported out of the vegetation zone, which was defined as the third stage. Therefore, the critical spatially averaged flow velocity in the third stage was adopted as the criterion for defining incipient sediment motion in vegetated open channel flow. This criterion was also used to investigate the incipient sediment motion in vegetated open channel flow in other studies[105-107].

2.3 *Predictive model for the incipient sediment motion*

The above analysis reveals that the rule of incipient sediment motion in vegetated open channel flow is remarkably different from that in non-vegetated open channel flow and requires a separate treatment. Considering the difficulty in using bed shear stress to judge incipient sediment motion in vegetated open channel flow, the critical flow velocity is more convenient and is routinely employed[24, 80-83, 85]. The experimental conditions and proposed models are summarized in Table 2.

From experiments conducted by Tang et al.[104], Yang et al.[112] considered incipient sediment motion in the flow with rigid emergent vegetation while Wang et al.[105], Xue et al.[106] explored the influence of submerged vegetation on the incipient motion of sediment. Unlike the other experiments, the vegetation was composed of thin rubber cylinders with a stiffness similar to that of flexible natural plants of the experiments by Wang et al.[105]. Moreover, they proposed to bridge the predictive model so that it can be applied to both rigid emergent and flexible submerged vegetation by considering the factors reflecting the winding level and submergence ratios of vegetation based on Tang et al.[104]. However, the model proposed by Wang et al.[105] did not satisfactorily described the data for submerged flexible vegetation. Furthermore, the model for incipient sediment motion in the flow with emergent rigid vegetation proposed by Tang et al.[104] must be treated as an empirical summary of their experiments. Xue et al.[106] focused on the incipient sediment motion in flow with rigid submerged vegetation. Through a series of experiments, they developed an empirical model to predict the critical flow velocity of incipient sediment motion with rigid submerged vegetation. The predicted critical velocities described well the experiments. However, the model may not be convenient in practice because it was based on averaged flow velocity below the vegetation height rather than the whole water depth (or bulk velocity).

It is widely accepted that the incipient motion of the sediments is due to the intense interactions between sediment grains and near-bed flow structure and turbulence statistics. Recent studies have shown that the spectral properties of turbulence dominate the local entertainment of sediment grains[113-114]. Similar mechanisms were also discussed in vegetated channels. Yang et al.[112] proposed a turbulent kinetic energy (TKE) model to predict the incipient sediment motion in vegetated open channel flow by assuming that the near-bed TKE sets the threshold of incipient sediment motion. Subsequently, the near-bed TKE was considered as the sum of the TKE generated by

Table 2 Summary of the predicting models for incipient sediment motion

Investigators	Vegetation parameters				Particle properties	Predicting model
	λ	d /mm	Pattern	Submergence	d_s /mm	
Tang et al.[104]	0.0047-0.014	6	Linear	Emergent	0.58, 0.67	$U_{pc}=0.36\sqrt{\frac{\gamma_s-\gamma}{\gamma}gd_s}\left(\frac{H}{d_s}\right)^{1/6}\left(\frac{d\sqrt{\frac{\pi}{4\lambda}-1}}{\sqrt{Hd_s}}\right)^{0.319}$
Wang et al.[105]	0.0057-0.0189	6	Linear	2.11-3.16	0.58, 0.67	$U_{pc}=0.36\sqrt{\frac{\gamma_s-\gamma}{\gamma}gd_s}\left(\frac{H}{d_s}\right)^{1/6}\left(\frac{d\sqrt{\frac{\pi}{4\lambda}-1}}{\sqrt{Hd_s}}\right)^{0.319}\left(\frac{h}{h_v}\right)^{3.5}\left(\frac{H}{h_v}\right)^{0.18}$
Yang et al.[112]	0.006-0.05	6.3	Staggered	Emergent	1.85, 0.73	$\frac{U_{pc}}{U_{c0}}=\frac{1}{\sqrt{1+C\lambda^{2/3}}}$, $C=\frac{0.9C_d^{2/3}}{C_b}$
Xue et al.[106]	0.011-0.031	8	Linear	1.2-2.03	0.5, 1	$U_{pc}=0.463\left[\left(\frac{dh}{Hd_s}\right)^{0.04}\left(\frac{\pi d}{4\lambda L_x}-1\right)^{0.29}\right]^{0.53}U_{c0}$ $U_{c0}=1.34\left(\frac{H}{d_s}\right)^{0.14}\left[\frac{\gamma_s-\gamma}{\gamma}gd_s+0.000000337\frac{10+H}{d_s^{0.72}}\right]^{1/2}$
Cheng et al.[102]	0.0047-0.014	6	Linear	Emergent	0.58, 0.67	$U_{pc}=\sqrt{\frac{\alpha}{1+\beta\lambda^{2/3}}}\sqrt{\frac{\gamma_s-\gamma}{\gamma}gd_s}$, $\alpha=5$, $\beta=28$
	0.006-0.05	6.3	Staggered		0.73, 1.85	
Wang et al.[115]	0.011-0.031	8	Linear	1.2-2.03	0.5, 1	$U_{pc}=1.34\left(\frac{H}{d_s}\right)^{1/7}\left[1-0.55(C_Dah_v)^{0.24}\right]\sqrt{\frac{\gamma_s-\gamma}{\gamma}gd_s}$
	0.0047-0.014	6	Linear	1.2-2.03	0.58, 0.67	
	0.006-0.05	6.3	Staggered		0.73, 1.85	

Note: Cheng et al.[102] did not conduct experiments here and their data were taken from Tang et al.[104] and Yang et al.[112]. The λ is vegetation density. The d and d_s are the vegetation stem diameter and the median diameter of particle, respectively. The $U_{p,c}$ is the critical double averaged pore flow velocities for the incipient sediment motion with vegetation, U_{c0} is the critical averaged flow velocities for the incipient sediment motion without vegetation. The h and h_v are the original height of vegetation and the height under the flow force respectively, and L_x is the distances between the centers of adjacent vegetation stems in the flow directions. The C_b is the bed roughness coefficient. The value of γ_s/γ is 2.65 for all researches listed in this table.

both river bed and vegetation. Finally, a prediction for the critical flow velocity of the incipient sediment motion was given by their model. Although their model was only applicable to sparse emergent vegetation, it unified the incipient sediment motion over the bare bed and in the vegetated channel. By integrating the influence of mean flow and turbulence on sediment motion and applying the spatiotemporal average to the force balance equation of the incipient sediment motion, Cheng et al.[102] developed a formula for the critical flow velocity in vegetated open channel flow. Although the determination of the drag coefficient of vegetation was avoided, two coefficients in the formula were calibrated by best fit to experiments reported by Yang et al.[112] and Tang et al.[104]. Recently, Wang et al.[115] developed another relation that accounted for vegetation drag in the incipient sediment motion formulation. The relation was shown to be in acceptable agreement with experiments. It was later extended to the case of submerged vegetation and successfully predicted Xue et al.[106] 's experiments on sediment incipient motion.

3. Sediment transport in vegetated channels

The spatial template for vegetation distribution in rivers usually follows riverbed elevation and decreases in suspended sediment concentration[116-118]. The latter is an indication of the effect of vegetation on sediment retention and water purification. Sediment transport, mainly including bed-load transport and suspended-load transport, is another focus given its significance to ecological function and is covered in this section

3.1 *Suspended-load transport*

The suspended-load transport rate is commonly derived by multiplying sediment transport velocity and suspended sediment concentration (SSC). It also can be obtained by directly determining the cross-sectional averaged value of SSC[119]. For rivers whose bed is covered by vegetation, the suspended transport velocity is approximated by the flow velocity given the small inertia of suspended particles (i.e., Stokes number much less than unity[120]). A logical first step to explore suspended-load transport rate is then the vertical distribution of SSC.

Sediment diffusion coefficient ε_s that indicates the effect of turbulent intensity induced by vegetation wake vortices in sediment-load flow was considered as a significant factor in suspended sediment transport. As for the determination of sediment diffusion coefficient, it is usually linked to the turbulent momentum diffusion coefficient ε_m via a turbulent Schmidt number St_c given as $\varepsilon_s = \varepsilon_m / St_c$ also written as $\varepsilon_s = \eta\varepsilon_m$, where $\eta = 1/St_c$. Sediment diffusion coefficients were mainly derived by fitting the vertical distribution of SSC to experiments[121-125] and deviations of η from unity linked to sediment or flow properties. The main results are listed in Table 3.

The variations in η are appreciable across experiments. Lv[121] conducted experiments with rigid cylinders to mimic natural vegetation in a laboratory flume. The sediment diffusion coefficient in vegetated channel flows was assumed similar to ε_m in non-vegetation channels. This assumption enabled an

Table 3 Summary of different expressions of the turbulent diffusion coefficient ε_m, the analytical solution of SSC vertical distribution in previous studies

References	ε_m	η	C
Lv[121]	$\kappa u_* z\dfrac{H-z}{H}$, $z<H$	0.77-1.65	$C=C_{a_1}\left(\dfrac{H-z}{z}\dfrac{a_1}{H-a_1}\right)^{\varpi_s/\eta\kappa u_*}$, $z<H$
Yang et al.[122]	$\begin{cases} z\dfrac{\kappa u_*}{C_u}\left(\dfrac{H-z}{H-h}\right), z\ge h \\ z\dfrac{\kappa u_*}{C_u}, z<h \end{cases}$	1	$C=\begin{cases} C_{a_1}\left(\dfrac{a_1}{z}\right)^{\varpi_s/\kappa u_*}\left(\dfrac{H-z}{z}\dfrac{h}{H-h}\right)^{[(H-h)/H](\varpi_s/\kappa u_*)}, z\ge h \\ C_{a_1}\left(\dfrac{a_1}{z}\right)^{\varpi_s/\kappa u_*}, z<h \end{cases}$
Li et al.[123]	$\begin{cases} \eta\dfrac{\kappa g S}{u_*}(H-z)(z-z_m), z>h \\ \eta\dfrac{gS(H-h)l}{\beta(u_h-u_1)}\mathrm{e}^{(\alpha-\beta/l)(z-h)}, z<h \end{cases}$	$1+1.56\left(\dfrac{\varpi_s}{u_*}\right)^2$	$\begin{cases} \ln\left(\dfrac{C}{C_h}\right)=-\dfrac{\varpi_s}{\eta g S}\dfrac{u_*}{\kappa}\dfrac{1}{H-z_m}\ln\dfrac{(z-z_m)(H-h)}{(H-z)(h-z_m)}, z>h \\ \ln\left(\dfrac{C_h}{C}\right)=-\dfrac{\varpi_s}{\eta g S}\dfrac{\beta}{\beta-\alpha l}\dfrac{u_h-u_1}{H-h}\left[1-\mathrm{e}^{(\beta/l-\alpha)(z-h)}\right], z<h \end{cases}$
Li et al.[124]	$\kappa u_*(z-d)\dfrac{H-z}{H-h}$, $z>h$	1.25	$C=C_{a_1}\left(\dfrac{H-z}{z-d}\dfrac{a_1-d}{H-a_1}\right)^{(\varpi_s/\eta\kappa u_*)[(H-h)/(H-d)]}$, $z>h$
Li et al.[125]	$\kappa u_* h\left(A\dfrac{z}{h}+B\right)$, $z>h$	1	$C=C_{a_1}\left(\dfrac{-A\kappa u_* z-B\kappa u_* h}{-A\kappa u_* a_1-B\kappa u_* h}\right)^{\varpi_s/(-A\eta\kappa u_*)}$, $z>h$

Note: C, C_{a1} and C_h are the SSC and SSC at the referenced height (a_1) and the top of the vegetation, respectively, ϖ_s is the settling velocity of sediment, z_m is the displacement height and $z_m = h-\delta_e/2$, l is the mixing length, u_h and u_1 are the velocity at the top of the vegetation and within the vegetated region, respectively, parameter β is set to u_*/u_h, α, C_u, A and B are constant, d is zero-plane-dispacement.

estimate of η by fitting an analytical solution of SSC to the data. Yang et al.[122] also derived vertical distribution of SSC with the same method as Lv[121] but used experiments from Yuuki and Okabe[126]. The main critique to this aforementioned approach is that the ε_m profile in vegetated channels is different from its non-vegetated counterpart[70] prompting alternative formulations. Huai et al.[127] and Li et al.[123] both proposed such alternative. They first optimized the expression for ε_m using prior studies for turbulent flow within vegetated systems and then fitted η to different experiments. Li et al.[124] conducted flume experiments on the vertical distribution of SSC in a channel with flexible vegetation. The flexible vegetation is more likely to represent the natural vegetation in rivers compared to rigid cylinders. However, they only interrogated the SSC profile over the vegetated section. Further studies on SSC and sediment diffusion characteristics were conducted in a channel covered by flexible vegetation with foliage. To explain these measured SSC profile shapes, they assumed $\eta = 1$ [125], which may be valid for fine sediments[128] in the limit of very small Stokes numbers. In the experiments of Li et al.[125], the SSC was small near the water surface and large near the riverbed. For within the vegetated region, the SSC profile decreased as a result that is different from the common profile patterns of suspended sediment over bare channels. The study of Huai et al.[129] emphasized that the dispersion effect of spatial heterogeneity reduced by the existence of vegetation played an important role in the suspended sediment transport. They generalized the dispersion coefficient formula in the region of vegetation while ignoring it in the non-vegetated region. They proposed an analytical solution to the SSC profile by integrating the sediment advection- diffusion equation with such a representation for dispersion. To what degree this approach or other generalizations can be successful awaits future experiments in which both velocity and sediments are simultaneously measured at high frequency to enable the estimation of turbulent fluxes and mean concentrations.

3.2 *Bed-load transport*

As noted earlier, bed-load transport capacity is diminished within the vegetated region because the bed shear stress is reduced. The bed-load transport rate models mainly depend on two theories: bed shear stress theory and TKE theory. Several representative equations for the bed-load transport rate based on these two theories are listed in Table 4.

In flow over bare bed, the sediment transport rate is calculated according to the bed shear stress[130] because the stress is considered as the criterion responsible for sediment onset movement (i.e., the Shields number). Most studies followed the bare-bed flow and extended applications to channels covered with vegetation by partitioning the total shear stress into three parts: the bed shear stress, the shear stress induced by vegetation[110, 131] and the grain-related stress inducing sediment particles transport[132]. From the summary of bed-load transport rate in the Table 4, the key problem in these models is how to determine the bed shear stress in vegetated channel flow. Although these studies provide a direction for the study of bed-load transport rate in vegetated channels, there is an obvious deficiency. These empirical formulae are derived from limited data sets and thus offer a summary for the conditions interrogated by the experiments. Briefly, Wu el al.[131] obtained a sediment transport rate equation by verifying a formula derived in rough river with experiments in a channel with vegetation. The formula of Jordanova and James[110] was derived from experiments on sediment transport rate with unchanged sediment size, stem diameter, and stem spacing, which restricts its general applicability.

Table 4 The formulae for bed-load transport rate based on different key parameters in channels with vegetation

Theory	Study	Bed-load transport rate
Bed shear stress theory	Einstein[130]	$Q_{s*}=\begin{cases}2.15e^{-0.391/\tau_*}, \tau_* < 0.18\\ 40\tau_*^3, 0.18 < \tau_* < 0.52\end{cases}$
	Wu el al.[131]	$Q_{s*}=0.0053\left[\left(\frac{n_b'}{n_b}\right)^{3/2}\frac{\tau_b}{\tau_c}-1\right]^{2.2}$
	Jordanova and James[110]	$Q_s=0.017(\tau_b-\tau_c)^{1.05}$
TKE theory	Yang and Nepf[134]	$Q_{s*}=\begin{cases}2.15e^{-2.06/k_{t*}}, k_{t*} < 0.95\\ 0.27k_{t*}^3, 0.95 < k_{t*} < 2.74\end{cases}$, dimensionless TKE: $k_{t*}=\frac{k_t}{(\rho_s/\rho-1)gd_s}$

Note: Q_s is the bed-load transport rate, τ_* is the dimensionless shear stress, Q_{s*} is the dimensionless bed-load transport rate, τ_b is the bed shear stress, τ_c is the critical bed shear stress, n_b is the Manning roughness coefficient of the channel bed, n_b' is the Manning roughness coefficient to the grain roughness, k_t is the turbulent kinetic energy, ρ_s represents the density of sediment, and d_s is the diameter of the sediment grain.

Recent studies indicated that turbulent kinetic energy may be a better criterion for onset of sediment motion when compared to bed shear stress[112, 133]. Unsurprisingly, studies on bed-load transport capacity in vegetated channels predicted by TKE followed[134-135]. The exploration of the effect of TKE on bed-load transport rate stimulated more experimental studies concerned with (1) sediment onset motion and (2) variation of TKE in vegetated channels. However, the knowledge gaps in elementary relations such as the relation between TKE and vegetation characteristics (density, structure, flexibility and

submergence) still persist. Clearly, barriers to progress on this front are due to (1) experimental difficulties in simultaneous measurements of flow and sediment concentration within vegetation and (2) a lack of general theories for flow and SSC within vegetated sections.

4. Sediment deposition and erosion in vegetated channels

The bed-load transport capacity can be diminished within the vegetation region as the bed shear stress is reduced by the absorption of momentum by drag on stem. Besides, sediment deposition and erosion impacts vegetation growth and spread in rivers by carrying organic materials attached to sediment particles[2]. Some studies clarified the feedback of vegetation growth with sediment deposition and erosion[3-5] prompting renewed interest in sediment deposition and erosion for river management.

In previous studies, two methods were mainly adopted to explore sediment deposition and erosion in laboratory experiments. One is feeding sediments at the upstream end of the flume and the other is paving a thick layer of sediments at the bottom of the flume. Discussions about erosion are less relevant in the former. For the latter, features of deposition and erosion can be studied though the experimental setup can impose constraints on the conclusions to be drawn.

For the condition of a thick layer of sediment positioned at the channel bottom, the profile of sediment will adjust according to the flow structure. The erosion occurs at the leading edge of the vegetation area because of the combined effect of vegetation blocking and updrafts, while the obvious deposition is observed in the latter half of vegetation patch[133, 136] or behind a patch, i.e., dune[87]. The vegetation density significantly impacts the deposition or erosion in the vegetated channel flow. The deposition within the latter half of a patch grows with the increase in vegetation density (see Fig. 7 in the article of Tinoco and Coco[133]). The study of Chen et al.[136] specifically showed that both the length and depth of scour decrease with increases in vegetation density. The dune height rises first and then is reduced with vegetation density increasing from sparse to dense.

The experiments conducted by feeding sediments in the upstream of cyclic flume are concerned with two aspects of sediment movement: the profile character of sediment deposition, and the influence of deposition patterns. In the following section, a discussion on the evolution and limitations of sediment deposition in vegetated channel flows is presented. In addition, we also discuss some research progress on bed-load transport rate in vegetated channels.

4.1 *Profile shape of sediment deposition*

The sediment deposition in vegetated channels varies with different kinds of vegetation such as finite vegetation patches and infinite vegetation. In fact, the infinite vegetation implies that the patch size is orders of magnitude longer in the direction of the flow than the adjustment distance as the flow encounters the vegetation patch (and thus all flow statistics are a function of z).

For the infinite vegetation approximation, experiments on sediment transport where sediments are fed upstream agree that in channels with submerged meadows, sediment deposition increases from the leading edge of vegetation and peaks near the position of the adjustment length $\sim(C_d a)^{-1}$. Beyond this point, a sharp decline in the transition region follows but then stabilizes at a small deposition in the developed region[137-138]. Although erosion did not occur as sediments were fed upstream of the channel, relative erosion occurred near the leading edge of the vegetation region compared with channels without vegetation (see Fig. 5 in article of Zhang et al.[137]).

When vegetation covers the half width of the river, not only the profile of deposition along the streamwise but also along the cross-section must be considered[139-142]. In these studies, some controversy appeared. For example, sediment deposition in the vegetation region is twice or triple as large as that in the region without vegetation[142]: however, in another experiment[140], the sediment deposition in the vegetated region is nearly the same as the non-vegetated region. One of the probable factors is the different types of vegetation used. Rigid cylinders were used in the study of Zong and Nepf[142] while flexible foliated vegetation were used by Box et al.[140]. The explicit reason for these differing experimental results is not clear and further elaboration still awaits.

4.2 *The primary controls on deposition patterns*

In a channel with an isolated vegetation patch, the sediment deposition and erosion are more complicated because of the variable flow velocity, vegetation densities and vegetation with or without foliage. In this section, a summary of the characteristic parameters impacting deposition and erosion in such channels is offered.

Firstly, the pattern of net sediment deposition in or near an isolated patch is closely related to the flow velocity[143]. The stem-scale turbulence, which dominates the sediment movement within the patch, is observed when the stem Reynolds number, $Re_p > 200$ [42, 144]. As the stem Reynolds number depends on the flow velocity and stem diameter, sediment transport within the patch based on these two factors is briefly reviewed. According to

experiments by Liu and Nepf[41], a non-uniform spatial distribution of net deposition was observed around and within the vegetation patch and the resuspension occurred in the bare channel when the flow velocity and the stem Reynolds number are high.

Vegetation density is another significant parameter controlling the deposition pattern in channels with isolated vegetation patches. Follett and Nepf[98] measured sediment patterns formed in a sand bed around circular patches of rigid cylinders with two patch densities (solid volume fraction 3% and 10%). Under the condition of sparse patch, sediment scoured from within the patch was mostly deposited within the distance of one patch diameter behind the patch. In the dense patch, sediment scoured from within the vegetation patch was deposited farther downstream because of the greater flow diversion (see Fig. 5 of Follett and Nepf[98]). The low density vegetation patch experienced a net deposition loss of fine sediment and organic materials within the patch[145], which indicated that the enhanced turbulence in the stem-scale led to the erosion of fine sediment in the patch. According to the characteristics of the sediment deposition and erosion within different density patches, the deposition of fine sediment was mainly observed behind the vegetation patch not inside the patch[146-147].

The sediment deposition characteristics show obvious differences between rigid emergent vegetation and flexible submerged vegetation. Sediment transport in channels with emergent vegetation patch[41, 98, 148] and submerged vegetation[91, 149-150] and their contrasts are now considered. In emergent vegetated channels, the strong updraft flow diminishes the deposition and even generates erosion in the leading edge of vegetation patch. The velocity and turbulence intensity are reduced in the wake region, and thus the enhanced deposition could be observed behind emergent vegetation patches, which results in a positive feedback promoting patch growth[41, 98]. However, the same feedback was reduced or completely absent in flexible submerged vegetated channels since the mean velocity and turbulence are almost not diminished[90]. This difference indicates that it may be much harder for flexible submerged vegetation patches to expand in space because the negative feedback inhibits patch growth. The implications of these results to river management are still being explored.

5. Interactions between vegetation dynamics and river morphodynamics

In the past, the influence of aquatic vegetation on river morphodynamics has usually been neglected. However, the temporal scales of river and vegetation evolution are not widely separated. This lack of time scale separation implies that river morphodynamics and vegetation dynamics cannot be modeled separately[151]. Although some qualitative and quantitative views have been proposed in recent years, the complex interactions between aquatic vegetation and river morphodynamics have not been unpacked. In this section, previous findings on the interaction between riparian vegetation and river morphodynamics are reviewed. Findings from numerical simulations that also describe such interactions are then presented.

5.1 *Influence of vegetation on river morphology*

In fact, each basic element of a river morphodynamics system is affected by riparian vegetation[152], including the flow field, turbulent structure, sediment transport and river bed evolution[70, 127, 129, 153-154]. Moreover, riparian vegetation has a significant influence on river bank strength, which may lead to river bank collapse or increased bank stabilization. Actually, the adjustment of the overall river morphology is caused by the combined effect of all of these factors[155-157]. This review explains the impact of vegetation on river morphology from three perspectives: bank, floodplain and river channel.

For river banks, erosion is mainly caused by three mechanisms: mass failure, fluvial scour and subaerial scour. The bank stability can be impacted by vegetation because of its positive and negative influence on geotechnical and hydrologic processes[8]. In terms of positive effects, the roots of vegetation can withstand high tensile stresses so that the bank material strength is increased to bear stronger shear resistance, which decreases the probability of mass failure[158]. Yu et al.[159] confirmed the effective reinforcement provided by riparian plant roots to unconsolidated banks by conducting in situ measurements in the Tarim River of China and using bank stability and toe erosion model to quantify the bank strength. However, strength gains are affected by different rooting conditions (length, density, and the soil medium). Reduction in flow velocity induced by vegetation also lowers scour rates, resulting in a decrease in erosion. Flexible vegetation, such as grasses or shrubs, have similar effects in reducing flow velocity to protect river banks from erosion[160]. As for negative effects, the existence of root strengthening near bank surfaces may lead to displacement of the failure surface and thus induce a larger pulse of sediment input into the river. Besides, root macropores do increase infiltration or add surcharge, which may cause reduction in bank stability[161].

It is widely known that deposition and erosion on floodplains are affected by overbank flow. However,

how riparian vegetation modifies sediment transport on floodplains is still not fully resolved in magnitude and sign[162-163]. Experiments and numerical model results suggest the sedimentation rates are higher when a floodplain is covered with vegetation[164-165]. Formulae to estimate rates of sediment deposition and erosion induced by vegetation have been proposed separately[166-168] and often treated in a disjointed manner. In terms of suspended sediment transport, it is usually modeled by adopting a simplified convection-diffusion equation when the flow is steady and longitudinally uniform. A depth-averaged vertical diffusivity and a depth-averaged transverse diffusivity are used to account for the effects of turbulence[169-170]. Formulae to predict vertical and transverse diffusivity have already been proposed that account for the effects of vegetation on the flow[23, 171].

How river channel shape (width and depth) evolves in response to the presence of vegetation has been a research focus for a long time[172-173]. Zen and Perona[174] found that interactions between riparian plants and water flow could control the evolution of river channel width and the adjustment of river channel trajectories. The influence of riparian vegetation on channel shapes has also been considered in some detail. Leopold and Wolman[7] related channel width (W) and depth (D) to the discharge (Q) using power-law relations of the form

$$W = m_1 Q^{n_1}, \quad H = m_2 Q^{n_2} \tag{7}$$

where m_1, m_2, n_1 and n_2 are empirical coefficients. Taking various vegetation types and density into account, different values of these four coefficients were proposed[175-177]. It was found that with a certain range of vegetation density, channel width decreases and channel depth increases while vegetation density increases[178]. However, in terms of W, Hey and Thorne[176] indicated that bed vegetation can widen a river channel because of increases in roughness causing a deflection of river flow onto the banks. Therefore, the effects of riparian vegetation on channel width needs further investigation. There are in-situ observations and data that reveal riparian vegetation plays an important role in changing river morphology into other types[156, 179-182]. For instance, Mackin[182] observed that the Wood River changes from braided to meandering while the bank vegetation changes from grasses to forest. The crucial role of riparian vegetation in river planform evolution could also be highlighted by the change of marked channel size, shape and pattern with vegetation removed[183]. A river channel can be progressively straightening and enlarging with river bed incision over decades after riparian and hillslope vegetation has been cleared[184].

5.2 *Influence of river morphodynamics on vegetation development*

River morphodynamics has influence on the growth and colonization of riparian vegetation. However, harsh and disturbed riparian environments in terms of inundation and susceptibility to drought, put higher demands on plants growing in such systems. As a result, plants that successfully colonize the riparian zone have the following characteristics: (1) producing a mass of seeds that can be easily spread, (2) resprouting after breakage or burial, and (3) tolerating extremely harsh conditions[185].

Riparian vegetation reproduction and colonization are dependent on a river's flow regime and flow structure, which facilitates transport of seeds and vegetative fragments to other reaches. It is widely known that the water level and flow regime are affected by seasons because of the amount of rainfall while seeds released by vegetation are also restricted by their growth cycle. Therefore, the area that riparian plants colonization is affected by fluvial processes[186].

Moving beyond flow regimes, channel form and the properties of bank soil are essential for aquatic vegetation spatial distribution and biomass dynamics since different plants have their own adaptability to river water level, bank soil moisture and nutrient conditions, inundation duration and frequency[187-189]. Thus, the horizontal distribution of vegetation in the riparian zone shows obvious community distribution difference such as species diversity, quantity and age structure[190-192]. For example, seedlings of vegetation tend to preferentially grow in horizontal bands on the inside of meander bends while younger plants choose specific locations where the surfaces of braided bars are relatively high to grow on braided rivers[193-194].

5.3 *Models*

In the past few decades, a number of quantitative models were proposed to elucidate the interaction between vegetation and river morphodynamics[195]. Millar[156] modified the criterion that is used to judge the transition between meandering and braided river by introducing the influence of aquatic vegetation.

At present, numerical models for the interaction between river flow and vegetation in multi-thread channels are not abundant[157, 196-198]. Most of these models proposed improvements in one aspect-introducing the dynamic growth of vegetation or the influence of vegetation roots on bank erosion. Both are logical starting points but do not offer any finality to them or all the remaining issues. Some models do not consider the floodplain morphodynamics dynamic so that they are not updated with riparian plants change. In terms of single-thread channels, several quantitative models are developed to represent river morphology changes and vegetation evolution, especially for meandering rivers[199-202]. In fact, the

proposed models can be divided into three types: (1) only considering the influence of riparian plants on river morphology[203], (2) only considering the impact of river flow on vegetation[204-205], (3) taking the interaction between river morphology and vegetation into account[206-208]. Furthermore, there are also minimalist models that consider the key factors or dynamics to obtain insightful analytical or semi-analytical solutions that could elaborate the quantitative relations among main variables[8]. The minimalist models are widely used in vegetation pattern formation, eco-hydrology and plant physiology. Recently, some minimalist models have also been developed to elucidate the influence of riparian vegetation ecosystems[209-211]. By comparing model outputs with data, such models could correctly identify the main processes in real rivers despite their simplicity, which is a promising first step.

6. Conclusions and future research challenges

This review summarized recent research results and highlighted how vegetation impacts river flow and sediment transport (on short-time scales) and river morphology (on long time scales). The effects of vegetation on flow and transport are discussed according to different criterion: emergent or submerged, rigid or flexible, sparse or dense, and finite or infinite vegetation patches. These classifications were introduced so as to modify established models and amend them for channels covered with plants. A single theory that accommodates all these criterion still awaits development, though experiments, simulations, and phenomenological understanding is rapidly progressing on this front. Different from non-vegetated channels, bed shear stress is no longer a suitable criterion for incipient sediment motion in channels covered with plants. The critical flow velocity and turbulent kinetic energy are both receiving more attention in this context. In terms of the interaction between vegetation and river morphology, there are both positive and negative feedbacks between them. Vegetation could indeed alter the river channel shape. Besides, in the past few decades, a large number of models were proposed to represent such interplay.

Quantitative models that describe vegetation influence on flow dynamics and sediment transport remain in their infancy. The plethora of physical mechanisms describing the interaction between vegetation and river morphology are also not fully understood and completely modeled synchronously. Clearly, any future research agenda on this topic must address the challenges highlighted below:

(1) Rigid cylinders are widely used in experiments to model vegetation, which could not represent all the characteristics of real vegetation in nature. Real plants have their distinct characteristics that differ across species. Thus, the model vegetation used in flume experiments must become more "realistic" so as to begin unpacking conveyance laws for real river systems that are urgently needed to support river restoration.

(2) Although there are large numbers of proposed formulae for sediment transport, most of them are empirical or semi-empirical. This level of empiricism is not surprising given that experiments reporting simultaneously velocity, sediment concentration, and sediment fluxes are scarce–especially inside vegetation. Clearly innovation in experimental techniques will be a priority to progress on new theories for sediment transport within vegetation.

(3) Future research should also focus on the relation between laboratory flume-scale flow and natural river-scale. In the absence of vegetation, matching the Froude number, the Reynolds number, and relative roughness (for high Reynolds numbers) allow scaling up from laboratory to natural conditions. Such clarity in the choice of dimensionless numbers that enables upscaling from "lab to river" remains lagging for rivers covered by vegetation.

(4) Much of the current understanding on the interaction between aquatic vegetation and flow is for flat or uniformly sloping terrain. The combined role of topography and vegetation on flow dynamics and sediment transport is also urgently needed. Only a handful of experiments considered flow over complex terrain covered by vegetation–and those have been restricted to a train of cosine shaped surfaces[212-217].

(5) To represent the interaction between vegetation and river morphology, present models have introduced a large number of (ad-hoc) parameters suffering from the much discussed equifinality problem[218]. How to by-pass the equifinality "curse" remains a challenge for the future, where undoubtedly hydro meteorological processes and human activities must be included.

Legend has it that Albert Einstein discouraged his son Hans Albert from exploring sediment transport because of the daunting challenges associated with turbulent phenomenon. Hans ignored this advice and went on to become a prominent scientist and engineer that shaped modern sediment-transport theory and its practice[219]. Research on flow dynamics and sediment transport in vegetated channels expands the path Hans charted by offering a multidisciplinary and fascinating topic for academicians and practitioners alike. As this review illustrates, it remains a fertile area for graduate student dissertations concerned with developing fundamentals, welding vast knowledge from distinct disciplines, and innovating experiments (lab and field or direct numerical simulations) in a manner that maintains high societal impact.

References

[1] Wang C., Zheng S. S., Wang P. F. et al. Interactions between vegetation, water flow and sediment transport: A review [J]. *Journal of Hydrodynamics*, 2015, 27(1): 24-37.

[2] Vandenbruwaene W., Temmerman S., Bouma T. J. et al. Flow interaction with dynamic vegetation patches: Implications for biogeomorphic evolution of a tidal landscape [J]. *Journal of Geophysical Research: Earth Surface*, 2011, 116: F1008.

[3] Cotton J. A., Wharton G., Bass J. A. B. et al. The effects of seasonal changes to in-stream vegetation cover on patterns of flow and accumulation of sediment [J]. *Geomorphology*, 2006, 77(3-4): 320-334.

[4] Vastila K., Jarvela J., Koivusalo H. Flow–vegetation–sediment interaction in a cohesive compound channel [J]. *Journal of Hydraulic Engineering, ASCE*, 2016, 142(1): 4015034.

[5] Yamasaki T. N., de Lima P. H. S., Silva D. F. et al. From patch to channel scale: The evolution of emergent vegetation in a channel [J]. *Advances in Water Resources*, 2019, 129: 131-145.

[6] Scheer A., Kruppke H., Heib R. River, coastal and estuarine morphodynamics [M]. Berlin Heidelberg, Germany: Springer, 2001.

[7] Leopold L. B., Wolman M. G. River channel patterns-braided, meandering, and straight [J]. *The Professional Geographer*, 1957, 9: 39-85.

[8] Camporeale C., Perucca E., Ridolfi L. et al. Modeling the interactions between river morphodynamics and riparian vegetation [J]. *Reviews of Geophysics*, 2013, 51(3): 379-414.

[9] Curran J. C., Hession W. C. Vegetative impacts on hydraulics and sediment processes across the fluvial system [J]. *Journal of Hydrology*, 2013, 505: 364-376.

[10] Poggi D., Porporato A., Ridolfi L. et al. The effect of vegetation density on canopy sub-layer turbulence [J]. *Boundary-Layer Meteorology*, 2004, 111(3): 565-587.

[11] Katul G., Wiberg P., Albertson J. et al. A mixing layer theory for flow resistance in shallow streams [J]. *Water Resources Research*, 2002, 38(11): 31-32.

[12] Gioia G., Bombardelli F. A. Scaling and similarity in rough channel flows [J]. *Physical Review Letters*, 2001, 88(1): 14501.

[13] Bonetti S., Manoli G., Manes C. et al. Manning's formula and Strickler's scaling explained by a co-spectral budget model [J]. *Journal of Fluid Mechanics*, 2017, 812: 1189.

[14] Crompton O., Katul G. G., Thompson S. Resistance formulations in shallow overland flow along a hillslope covered with patchy vegetation [J]. *Water Resources Research*, 2020, 56(5): e2020WR27194.

[15] Martyushev L. M. Some interesting consequences of the maximum entropy production principle [J]. *Journal of Experimental and Theoretical Physics*, 2007, 104(4): 651-654.

[16] Wu Y. J., Jing H. F., Li C. G. et al. Flow characteristics in open channels with aquatic rigid vegetation [J]. *Journal of Hydrodynamics*, 2020, 32(6): 1100-1108.

[17] Wang W. J., Peng W. Q., Huai W. X. et al. Roughness height of submerged vegetation in flow based on spatial structure [J]. *Journal of Hydrodynamics*, 2018, 30(4): 754-757.

[18] Wang W. J., Cui X. Y., Dong F. et al. Predictions of bulk velocity for open channel flow through submerged vegetation [J]. *Journal of Hydrodynamics*, 2020, 32(4): 795-799.

[19] Wooding R. A., Bradley E. F., Marshall J. K. Drag due to regular arrays of roughness elements of varying geometry [J]. *Boundary-Layer Meteorology*, 1973, 5(3): 285-308.

[20] Melis M., Poggi D., Fasanella G. et al. Resistance to flow on a sloping channel covered by dense vegetation following a dam break [J]. *Water Resources Research*, 2019, 55(2): 1040-1058.

[21] Tanino Y., Nepf H. M. Laboratory investigation of mean drag in a random array of rigid, emergent cylinders [J]. *Journal of Hydraulic Engineering, ASCE*, 2008, 134(1): 34-41.

[22] Liu M., Huai W., Yang Z. et al. A genetic programming-based model for drag coefficient of emergent vegetation in open channel flows [J]. *Advances in Water Resources*, 2020, 140: 103582.

[23] Nepf H. M. Drag, turbulence, and diffusion in flow through emergent vegetation [J]. *Water Resources Research*, 1999, 35(2): 479-489.

[24] D'Ippolito A., Calomino F., Alfonsi G. et al. Flow resistance in open channel due to vegetation at reach scale: A review [J]. *Water*, 2021, 13(2): 116.

[25] Koch D. L., Ladd A. J. C. Moderate Reynolds number flows through periodic and random arrays of aligned cylinders [J]. *Journal of Fluid Mechanics*, 1997, 349: 31-66.

[26] Etminan V., Lowe R. J., Ghisalberti M. A new model for predicting the drag exerted by vegetation canopies [J]. *Water Resources Research*, 2017, 53(4): 3179-3196.

[27] Nepf H. M. Hydrodynamics of vegetated channels [J]. *Journal of Hydraulic Research*, 2012, 50(3): 262-279.

[28] Katul G. G., Poggi D., Ridolfi L. A flow resistance model for assessing the impact of vegetation on flood routing mechanics [J]. *Water Resources Research*, 2011, 47: W8533.

[29] Konings A. G., Katul G. G., Thompson S. E. A phenomenological model for the flow resistance over submerged vegetation [J]. *Water Resources Research*, 2012, 48: W2522.

[30] Luhar M., Nepf H. M. From the blade scale to the reach scale: A characterization of aquatic vegetative drag [J]. *Advances in Water Resources*, 2013, 51: 305-316.

[31] Poggi D., Krug C., Katul G. G. Hydraulic resistance of submerged rigid vegetation derived from first-order closure models [J]. *Water Resources Research*, 2009, 45: W10442.

[32] Chanson H. Hydraulics of open channel flow [M]. Rotterdam, The Netherlands: Elsevier, 2004.

[33] Li S., Huai W. United formula for the friction factor in the turbulent region of pipe flow [J]. *PloS one*, 2016, 11(5): e154408.

[34] Li S. L., Shi H. R., Xue W. Y. et al. United friction resistance in open channel flows [J]. *Journal of Hydrodynamics*, 2015, 27(3): 469-472.

[35] Cheng N. S., Nguyen H. T. Hydraulic radius for evaluating resistance induced by simulated emergent vegetation in open-channel flows [J]. *Journal of Hydraulic Engineering, ASCE*, 2011, 137(9): 995-1004.

[36] van Rooijen A., Lowe R., Ghisalberti M. et al. Predicting current-induced drag in emergent and submerged aquatic vegetation canopies [J]. *Frontiers in Marine Science*, 2018, 5: 449.

[37] Cheng N. S. Representative roughness height of submerged vegetation [J]. *Water Resources Research*, 2011, 47: W08517.

[38] Li S., Shi H., Xiong Z. et al. New formulation for the

effective relative roughness height of open channel flows with submerged vegetation [J]. *Advances in Water Resources*, 2015, 86: 46-57.
[39] Yang F., Huai W., Zeng Y. New dynamic two-layer model for predicting depth-averaged velocity in open channel flows with rigid submerged canopies of different densities [J]. *Advances in Water Resources*, 2020, 138: 103553.
[40] Tang H., Tian Z., Yan J. et al. Determining drag coefficients and their application in modelling of turbulent flow with submerged vegetation [J]. *Advances in Water Resources*, 2014, 69: 134-145.
[41] Liu C., Nepf H. M. Sediment deposition within and around a finite patch of model vegetation over a range of channel velocity [J]. *Water Resources Research*, 2016, 52: 600-612.
[42] Tanino Y., Nepf H. M. Lateral dispersion in random cylinder arrays at high Reynolds number [J]. *Journal of Fluid Mechanics*, 2008, 600: 339-371.
[43] Raupach M. R., Shaw R. H. Averaging procedures for flow within vegetation canopies [J]. *Boundary-Layer Meteorology*, 1982, 22(1): 79-90.
[44] Chang K, Constantinescu G. Numerical investigation of flow and turbulence structure through and around a circular array of rigid cylinders [J]. *Journal of Fluid Mechanics*, 2015, 776: 161-199.
[45] Poggi D., Katul G. G., Albertson J. D. A note on the contribution of dispersive fluxes to momentum transfer within canopies [J]. *Boundary-Layer Meteorology*, 2004, 111(3): 615-621.
[46] Poggi D., Katul G. G. The effect of canopy roughness density on the constitutive components of the dispersive stresses [J]. *Experiments in Fluids*, 2008, 45(1): 111-121.
[47] Huthoff F., Augustijn D. C., Hulscher S. J. Analytical solution of the depth-averaged flow velocity in case of submerged rigid cylindrical vegetation [J]. *Water Resources Research*, 2007, 43(6): 6413.
[48] Liu D., Diplas P., Fairbanks J. D. et al. An experimental study of flow through rigid vegetation [J]. *Journal of Geophysical Research: Earth Surfac*e, 2008, 113(F4): F04015.
[49] Stoesser T., Kim S. J., Diplas P. Turbulent flow through idealized emergent vegetation [J]. *Journal of Hydraulic Engineering, ASCE*, 2010, 136(12): 1003-1017.
[50] Raupach M. R., Finnigan J. J., Brunei Y. Coherent eddies and turbulence in vegetation canopies: The mixing-layer analogy [J]. *Boundary Layer Meteorology*, 1996, 78(3-4): 351-382.
[51] Huai W. X., Zhang J., Katul G. G. et al. The structure of turbulent flow through submerged flexible vegetation [J]. *Journal of Hydrodynamics*, 2019, 31(2): 274-292.
[52] Chen Z., Jiang C., Nepf H. Flow adjustment at the leading edge of a submerged aquatic canopy [J]. *Water Resources Research*, 2013, 49(9): 5537-5551.
[53] Ghisalberti M., Nepf H. M. The limited growth of vegetated shear layers [J]. *Water Resources Research*, 2004, 40(7): W07502.
[54] Tang X. Evaluating two-layer models for velocity profiles in open-channels with submerged vegetation [J]. *Journal of Geoscience and Environment Protection*, 2019, 7(1): 68-80.
[55] Okamoto T. A., Nezu I. Large eddy simulation of 3-D flow structure and mass transport in open-channel flows with submerged vegetations [J]. *Journal of Hydro-Environment Research*, 2010, 4(3): 185-197.
[56] Stoesser T., Salvador G. P., Rodi W. et al. Large eddy simulation of turbulent flow through submerged vegetation [J]. *Transport in Porous Media*, 2009, 78: 347-365.
[57] Stoesser T., Liang C. C., Rodi W. et al. Large eddy simulation of fully-developed turbulent flow through submerged vegetation (Alves E. C. T. L., Cardoso A. H., Leal J. G. A. B. et al. River flow) [M]. New York, USA: Taylor and Francis, 2006, 227-234.
[58] Wang Y. Q., Yu H. D., Zhao W. W. et al. Liutex-based vortex control with implications for cavitation suppression [J]. *Journal of Hydrodynamics*, 2021, 33(1): 74-85.
[59] Zhao W. W., Wang Y. Q., Chen S. T. et al. Parametric study of Liutex-based force field models [J]. *Journal of Hydrodynamics*, 2021, 33(1): 86-92.
[60] Winant C. D., Browand F. K. Vortex pairing: The mechanism of turbulent mixing-layer growth at moderate Reynolds number [J]. *Journal of Fluid Mechanics*, 1974, 63: 237-255.
[61] Nepf H., Ghisalberti M., White B. et al. Retention time and dispersion associated with submerged aquatic canopies [J]. *Water Resources Research*, 2007, 43(4): W04422.
[62] Okamoto T. A., Nezu I. Spatial evolution of coherent motions in finite-length vegetation patch flow [J]. *Environmental Fluid Mechanics*, 2013, 13(5): 417-434.
[63] Nepf H. M., Vivoni E. R. Flow structure in depth-limited, vegetated flow [J]. *Journal of Geophysical Research Oceans*, 2000, 105(C12): 28547-28557.
[64] Okamoto T. A., Nezu I. Turbulence structure and "Monami" phenomena in flexible vegetated open-channel flows [J]. *Journal of Hydraulic Research*, 2009, 47(6): 798-810.
[65] Belcher S. E., Jerram N., Hunt J. C. R. Adjustment of a turbulent boundary layer to a canopy of roughness elements [J]. *Journal of Fluid Mechanics*, 2003, 488: 369-398.
[66] Huai W. X., Zeng Y. H., Xu Z. G. et al. Three-layer model for vertical velocity distribution in open channel flow with submerged rigid vegetation [J]. *Advances in Water Resources*, 2009, 32(4): 487-492.
[67] Cheng N. S., Nguyen H. T., Tan S. K. et al. Scaling of velocity profiles for depth-limited open channel flows over simulated rigid vegetation [J]. *Journal of Hydraulic Engineering, ASCE*, 2012, 138(8): 673-683.
[68] Huai W., Wang W., Hu Y. et al. Analytical model of the mean velocity distribution in an open channel with double-layered rigid vegetation [J]. *Advances in Water Resources*, 2014, 69: 106-113.
[69] Huai W. X., Chen Z. B., Han J. et al. Mathematical model for the flow with submerged and emerged rigid vegetation [J]. *Journal of Hydrodynamic*s, 2009, 21(5): 722-729.
[70] Nepf H. M. Flow and transport in regions with aquatic vegetation [J]. *Annual Review of Fluid Mechanics*, 2012, 44: 123-142.
[71] Afzal M., Arslan M., Müller J. A. et al. Floating treatment wetlands as a suitable option for large-scale wastewater treatment [J]. *Nature Sustainability*, 2019, 2(9): 863-871.
[72] Li S., Katul G. Contaminant removal efficiency of floating treatment wetlands [J]. *Environmental Research Letters*, 2020, 15(10): 1040b7.
[73] Wang H., Li S., Zhu Z. et al. Analyzing solute transport in modeled wetland flows under surface wind and bed absorption conditions [J]. *International Journal of Heat and Mass Transfer*, 2020, 150: 119319.
[74] Ai Y. D., Liu M. Y., Huai W. X. Numerical investigation of flow with floating vegetation island [J]. *Journal of Hydrodynamics*, 2020, 32(1): 31-43.

[75] Fu X., Wang F., Liu M. et al. Analysis of turbulent flow structures in the straight rectangular open channel with floating vegetated islands [J]. *Environmental Science and Pollution Research*, 2020, 27: 26856-26867.
[76] Plew D. R. Depth-averaged drag coefficient for modeling flow through suspended canopies [J]. *Journal of Hydraulic Engineering, ASCE*, 2011, 137(2): 234-247.
[77] Cheng W., Sun Z., Liang S. Numerical simulation of flow through suspended and submerged canopy [J]. *Advances in Water Resources*, 2019, 127: 109-119.
[78] Li S., Katul G., Huai W. Mean velocity and shear stress distribution in floating treatment wetlands: An analytical study [J]. *Water Resources Research*, 2019, 55(8): 6436-6449.
[79] Huai W., Hu Y., Zeng Y. et al. Velocity distribution for open channel flows with suspended vegetation [J]. *Advances in Water Resources*, 2012, 49: 56-61.
[80] Li Q., Zeng Y. H., Bai Y. Mean flow and turbulence structure of open channel flow with suspended vegetation [J]. *Journal of Hydrodynamics*, 2020, 32(2): 314-325.
[81] Yu W. Y., Jiang C. B., Shi Y. et al. Experimental study of the impact of the floating-vegetation island on mean and turbulence structure [J]. *Journal of Hydrodynamics*, 2019, 31(5): 922-930.
[82] Zhao F., Huai W., Li D. Numerical modeling of open channel flow with suspended canopy [J]. *Advances in Water Resources*, 2017, 105: 132-143.
[83] Cheng N. S., Hui C. L., Chen X. Estimate of drag coefficient for a finite patch of rigid cylinders [J]. *Journal of Hydraulic Engineering, ASCE*, 2019, 145(2): 6018019.
[84] Gong Y., Stoesser T., Mao J. et al. LES of flow through and around a finite patch of thin plates [J]. *Water Resources Researc*h, 2019, 55(9): 7587-7605.
[85] Zhang J., Liang D., Fan X. et al. Detached eddy simulation of flow through a circular patch of free-surface-piercing cylinders [J]. *Advances in Water Resources*, 2019, 123(800): 96-108.
[86] Li W. Q., Wang D., Jiao J. L. et al. Effects of vegetation patch density on flow velocity characteristics in an open channel [J]. J*ournal of Hydrodynamics*, 2019, 31(5): 1052-1059.
[87] Gu J., Shan Y., Liu C. et al. Feedbacks of flow and bed morphology from a submerged dense vegetation patch without upstream sediment supply [J]. *Environmental Fluid Mechanics*, 2019, 19(2): 475-493.
[88] Chang K., Constantinescu G., Park S. 2-D eddy resolving simulations of flow past a circular array of cylindrical plant stems [J]. *Journal of Hydrodynamics*, 2018, 30(2): 317-335.
[89] Taddei S., Manes C., Ganapathisubramani B. Characterisation of drag and wake properties of canopy patches immersed in turbulent boundary layers [J]. *Journal of Fluid Mechanics*, 2016, 798: 27-49.
[90] Ortiz A. C., Ashton A., Nepf H. Mean and turbulent velocity fields near rigid and flexible plants and the implications for deposition [J]. *Journal of Geophysical Research: Earth Surface*, 2013, 118(4): 2585-2599.
[91] Tanaka N., Yagisawa J. Flow structures and sedimentation characteristics around clump-type vegetation [J]. *Journal of Hydro-environment Research*, 2010, 4: 15-25.
[92] Zong L., Nepf H. Vortex development behind a finite porous obstruction in a channel [J]. *Journal of Fluid Mechanics*, 2012, 691: 368-391.
[93] Nicolle A., Eames I. Numerical study of flow through and around a circular array of cylinders [J]. *Journal of Fluid Mechanics*, 2011, 679: 1-31.
[94] Chang W. Y., Constantinescu G., Tsai W. F. Effect of array submergence on flow and coherent structures through and around a circular array of rigid vertical cylinders [J]. *Physics of Fluids*, 2020, 32(3): 35110.
[95] Nicolai C., Taddei S., Manes C. et al. Wakes of wall-bounded turbulent flows past patches of circular cylinders [J]. *Journal of Fluid Mechanics*, 2020, 892: A37.
[96] Liu M., Huai W., Ji B. Characteristics of the flow structures through and around a submerged canopy patch [J]. *Physics of Fluid*s, 2021, 33(3): 35144.
[97] Chang W. Y., Constantinescu G., Tsai W. F. On the flow and coherent structures generated by a circular array of rigid emerged cylinders placed in an open channel with flat and deformed bed [J]. *Journal of Fluid Mechanics*, 2017, 831: 1-40.
[98] Follett E. M., Nepf H. M. Sediment patterns near a model patch of reedy emergent vegetation [J]. *Geomorphology*, 2012, 179: 141-151.
[99] Chien N., Wan Z. Mechanics of sediment transport [M]. Reston, USA: American Society of Civil Engineers, 1999.
[100] Leonard L. A., Luther M. E. Flow hydrodynamics in tidal marsh canopies [J]. *Limnol Oceanogr*, 1995, 40(8): 1474-1484.
[101] Shi Z., Pethick J. S., Pye K. Flow structure in and above the various heights of a saltmarsh canopy: A laboratory flume study [J]. *Journal of Coastal Research*, 1995, 11(4): 1204-1209.
[102] Cheng N., Wei M., Lu Y. Critical flow velocity for incipient sediment motion in open channel flow with rigid emergent vegetation [J]. *Journal of Engineering Mechanics*, 2020, 146(11): 4020123.
[103] Bouma T. J., van Duren L. A., Temmerman S. et al. Spatial flow and sedimentation patterns within patches of epibenthic structures: Combining field, flume and modelling experiments [J]. *Continental Shelf Research*, 2007, 27(8): 1020-1045.
[104] Tang H. W., Wang H., Liang D. F. et al. Incipient motion of sediment in the presence of emergent rigid vegetation [J]. *Journal of Hydro-Environment Research*, 2013, 7(3): 202-208.
[105] Wang H., Tang H. W., Zhao H. Q. et al. Incipient motion of sediment in presence of submerged flexible vegetation [J]. *Water Science and Engineering*, 2015, 8(1): 63-67.
[106] Xue W., Wu S., Wu X. et al. Sediment incipient motion on movable bed in rigid vegetation environment [J]. *Advances in Water Science*, 2017, 28(6): 849-857.
[107] Shahmohammadi R., Afzalimehr H., Sui J. Impacts of turbulent flow over a channel bed with a vegetation patch on the incipient motion of sediment [J]. *Canadian Journal of Civil Engineering*, 2018, 45(9): 803-816.
[108] Watanabe K., Nagy H. M., Noguchi H. Flow structure and bed-load transport in vegetation flow [C]. *Advances in Hydraulics and Water Engineering-Proceedings of the 13th IAHR-APD Congress*, Singapore, 2002.
[109] Raupach M. R. Drag and drag partition on rough surfaces [J]. *Boundary-Layer Meteorology*, 1992, 60(4): 375-395.
[110] Jordanova A. A., James C. S. Experimental study of bed load transport through emergent vegetation [J]. *Journal of Hydraulic Engineering, ASCE*, 2003, 129(6): 474-478.
[111] Kothyari U. C., Hashimoto H., Hayashi K. Effect of tall vegetation on sediment transport by channel flows [J]. *Journal of Hydraulic Research*, 2009, 47(6): 700-710.
[112] Yang J. Q., Chung H., Nepf H. M. The onset of sediment transport in vegetated channels predicted by turbulent kinetic energy [J]. *Geophysical Research Letters*, 2016, 43(21): 112261-11268.

[113] Ali S. Z., Dey S. Origin of the scaling laws of sediment transport [J]. *Proceedings of the Royal Society A: Mathematical, Physical and Engineering Sciences*, 2017, 473(2197): 20160785.
[114] Li S., Katul G. Cospectral budget model describes incipient sediment motion in turbulent flows [J]. *Physical Review Fluids*, 2019, 4(9): 93801.
[115] Wang X., Huai W., Cao Z. An improved formula for incipient sediment motion in vegetated open channel flows [J]. *International Journal of Sediment Research*, 2021(in Press).
[116] Zhang Y., Lai X., Zhang L. et al. The influence of aquatic vegetation on flow structure and sediment deposition: A field study in Dongting Lake, China [J]. *Journal of Hydrology*, 2020, 584: 124644.
[117] Yang S. L. The role of scirpus marsh in attenuation of hydrodynamics and retention of fine sediment in the Yangtze Estuary [J]. *Estuarine, Coastal and Shelf Science*, 1998, 47(2): 227-233.
[118] Gruber R. K., Kemp W. M. Feedback effects in a coastal canopy-forming submersed plant bed [J]. *Limnology and Oceanography*, 2010, 55(6): 2285-2298.
[119] Huai W. X., Wang X., Guo Y. et al. Investigation of the sediment transport capacity in vegetated open channel flow [J]. *Journal of Hydrodynamic*s, 2021, 33(2): 386-389.
[120] Richter D., Chamecki M. Inertial effects on the vertical transport of suspended particles in a turbulent boundary layer [J]. *Boundary-Layer Meteorology*, 2018, 167(2): 235-256.
[121] Lv S. Q. Experimental study on distribution law of suspended sediment in water flow of rigid plants [D]. Nanjing, China: Hohai University, 2008(in Chinese).
[122] Yang W., Choi S. A two-layer approach for depth-limited open-channel flows with submerged vegetation [J]. *Journal of Hydraulic Research*, 2010, 48(4): 466-475.
[123] Li D., Yang Z., Sun Z. et al. Theoretical model of suspended sediment concentration in a flow with submerged vegetation [J]. *Water*, 2018, 10(11): 1656.
[124] Li Y., Xie L., Su T. Vertical distribution of suspended sediments above dense plants in water flow [J]. *Water*, 2020, 12(1): 12.
[125] Li Y., Xie L., Su T. C. Profile of suspended sediment concentration in submerged vegetated shallow water flow [J]. *Water Resources Research*, 2020, 56(4): e2019WR025551.
[126] Yuuki W., Okabe T. Hydrodynamic mechanism of suspended load on riverbeds vegetated by woody plants [J]. *Proceeding of Hydraulic Engineering*, 2002, 46: 701-706.
[127] Huai W., Yang L., Wang W. J. et al. Predicting the vertical low suspended sediment concentration in vegetated flow using a random displacement model [J]. *Journal of Hydrology*, 2019, 578: 124101.
[128] Absi R. Concentration profiles for fine and coarse sediments suspended by waves over ripples: An analytical study with the 1-DV gradient diffusion model [J]. *Advances in Water Resources*, 2010, 33(4): 411-418.
[129] Huai W., Yang L, Guo Y. Analytical solution of suspended sediment concentration profile: relevance of dispersive flow term in vegetated channels [J]. *Water Resources Researc*h, 2020, 56(7): e2019WR027012.
[130] Einstein H. A. The bed-load function for sediment transportation in open channel flows [M]. Washington DC, USA: US Department of Agriculture, 1950.
[131] Wu W., He Z. Effects of vegetation on flow conveyance and sediment transport capacity [J]. *International Journal of Sediment Research*, 2009, 24(3): 247-259.
[132] Le Bouteiller C., Venditti J. G. Sediment transport and shear stress partitioning in a vegetated flow [J]. *Water Resources Research*, 2015, 51(4): 2901-2922.
[133] Tinoco R. O., Coco G. A laboratory study on sediment resuspension within arrays of rigid cylinders [J]. *Advances in Water Resources*, 2016, 92: 1-9.
[134] Yang J. Q., Nepf H M. A Turbulence-based bed-load transport model for bare and vegetated channels [J]. *Geophysical Research Letters*, 2018, 45(19): 10410-428436.
[135] Yang J. Q., Nepf H. M. Impact of vegetation on bed load transport rate and bedform characteristics [J]. *Water Resources Research*, 2019, 55(7): 6109-6124.
[136] Chen S., Chan H., Li Y. Observations on flow and local scour around submerged flexible vegetation [J]. *Advances in Water Resources*, 2012, 43: 28-37.
[137] Zhang J., Lei J., Huai W. et al. Turbulence and particle deposition under steady flow along a submerged seagrass meadow [J]. *Journal of Geophysical Research: Oceans*, 2020,125(5): e2019JC015985.
[138] Follett E., Nepf H. Particle retention in a submerged meadow and its variation near the leading edge [J]. *Estuaries and Coasts*, 2018, 41(3): 724-733.
[139] Västilä K., Järvelä J. Characterizing natural riparian vegetation for modeling of flow and suspended sediment transport [J]. *Journal of Soils and Sediments*, 2018, 18(10): 3114-3130.
[140] Box W., Västilä K., Järvelä J. The interplay between flow field, suspended sediment concentration, and net deposition in a channel with flexible bank vegetation [J]. *Water*, 2019, 11(11): 2250.
[141] Kim H. S., Kimura I., Shimizu Y. Experiment and computation of morphological response to a vegetation patch in open-channel flows with erodible banks [J]. *Water*, 2019, 11(11): 2255.
[142] Zong L., Nepf H. Flow and deposition in and around a finite patch of vegetation [J]. *Geomorphology*, 2010, 116(3-4): 363-372.
[143] Fonseca M. S., Zieman J. C., Thayer G. W. et al. The role of current velocity in structuring eelgrass (Zostera marina L.) meadowsa [J]. *Estuarine, Coastal and Shelf Science*, 1983, 17(4): 367-380.
[144] Naden P., Rameshwaran P., Mountford O. et al. The influence of macrophyte growth, typical of eutrophic conditions, on river flow velocities and turbulence production [J]. *Hydrological Processes*, 2006, 20(18): 3915-3938.
[145] van Katwijk M. M., Bos A. R., Hermus D. C. R. et al. Sediment modification by seagrass beds: Muddification and sandification induced by plant cover and environmental conditions [J]. *Estuarine, Coastal and Shelf Science*, 2010, 89(2): 175-181.
[146] Tsujimoto T. Fluvial processes in streams with vegetation [J]. *Journal of Hydraulic Research*, 1999, 37(6): 789-803.
[147] Takemura T., Tanaka N. Flow structures and drag characteristics of a colony-type emergent roughness model mounted on a flat plate in uniform flow [J]. *Fluid Dynamics Research*, 2007, 39(9-10): 694-710.
[148] Shi Y., Jiang B., Nepf H. M. Influence of particle size and density, and channel velocity on the deposition patterns around a circular patch of model emergent vegetation [J]. *Water Resources Research*, 2016, 52(2): 1044-1055.

[149] Hu Z., Lei J., Liu C. et al. Wake structure and sediment deposition behind models of submerged vegetation with and without flexible leaves [J]. *Advances in Water Resources*, 2018, 118: 28-38.
[150] Liu C., Hu Z., Lei J. et al. Vortex structure and sediment deposition in the wake behind a finite patch of model submerged vegetation [J]. *Journal of Hydraulic Engineering, ASCE*, 2018, 144(2): 4017065.
[151] Phillips J. D. Biogeomorphology and landscape evolution: The problem of scale [J]. *Geomorphology*, 1995, 13(1-4): 337-347.
[152] Gibling M. R., Davies N. S. Palaeozoic landscapes shaped by plant evolution [J]. *Nature Geoscience*, 2012, 5(2): 99-105.
[153] Politti E., Bertoldi W., Gurnell A. et al. Feedbacks between the riparian Salicaceae and hydrogeomorphic processes: A quantitative review [J]. *Earth-Science Reviews*, 2018, 176: 147-165.
[154] Thorne C. R. Channel types and morphological classification (Applied fluvial geomorphology for river engineering and management) [M]. New York, USA: John Wiley and Sons, 1997.
[155] Allmendinger N. E., Pizzuto J. E., Potter N. et al. The influence of riparian vegetation on stream width, eastern Pennsylvania, USA [J]. *Bulletin of the Geological Society of America*, 2005, 117(1-2): 229-243.
[156] Millar R. G. Influence of bank vegetation on alluvial channel patterns [J]. *Water Resources Research*, 2000, 36(4): 1109-1118.
[157] Murray B. A., Paola C. Modelling the effect of vegetation on channel pattern in bedload rivers [J]. *Earth Surface Processes and Landforms*, 2003, 28(2): 131-143.
[158] Pollen N., Simon A., Collison A. et al. Advances in assessing the mechanical and hydrologic effects of riparian vegetation on streambank stability: Riparian Vegetation and Fluvial Geomorphology, 2004 [M]. Washington DC, USA: American Geophysical Union, 2004.
[159] Yu G. A., Li Z., Yang H. et al. Effects of riparian plant roots on the unconsolidated bank stability of meandering channels in the Tarim River, China [J]. *Geomorphology*, 2020, 351: 106958.
[160] Trimble S. W. Stream channel erosion and change resulting from riparian forests [J]. *Geology*, 1997, 25(5): 467-469.
[161] Simon A., Collison A. J. C. Quantifying the mechanical and hydrologic effects of riparian vegetation on streambank stability [J]. *Earth Surface Processes and Landforms*, 2002, 27(5): 527-546.
[162] Nicholas A. P., Mitchell C. A. Numerical simulation of overbank processes in topographically complex floodplain environments [J]. *Hydrological Processes*, 2003, 17(4): 727-746.
[163] Steiger J., Gurnell A. M., Ergenzinger P. et al. Sedimentation in the riparian zone of an incising river [J]. *Earth Surface Processes and Landforms: The Journal of the British Geomorphological Research Group*, 2001, 26(1): 91-108.
[164] Croissant T., Lague D., Davy P. Channel widening downstream of valley gorges influenced by flood frequency and floodplain roughness [J]. *Journal of Geophysical Research: Earth Surface*, 2019, 124(1): 154-174.
[165] Nanson G. C., Beach H. F. Forest succession and sedimentation on a meandering-river floodplain, northeast British Columbia, Canada [J]. *Journal of Biogeography*, 1977, 4(3): 229-251.
[166] Collins D. B. G., Bras R. L., Tucker G. E. Modeling the effects of vegetation-erosion coupling on landscape evolution [J]. *Journal of Geophysical Research-Earth Surface*, 2004, 109(F3): F03004 .
[167] D′Alpaos A., Lanzoni S. Evoluzione morfodinamica a lungo termine della sezione trasversale di canali a marea [C]. *XXX Convegno di Idraulica e Costruzioni Idrauliche*, Roma, Italy, 2006.
[168] Palmer M. R., Nepf H. M., Pettersson T. J. R. et al. Observations of particle capture on a cylindrical collector: Implications for particle accumulation and removal in aquatic systems [J]. *Limnology and Oceanography*, 2004, 49(1): 76-85.
[169] Ikeda S., Izumi N., Ito R. Effects of pile dikes on flow retardation and sediment transport [J]. *Journal of Hydraulic Engineering, ASCE*, 1991, 117(11): 1459-1478.
[170] James C. S. Sediment transfer to overbank sections [J]. *Journal of Hydraulic Research*, 1985, 23(5): 435-452.
[171] Elliott A. H. Settling of fine sediment in a channel with emergent vegetation [J]. *Journal of Hydraulic Engineering, ASCE*, 2000, 126(8): 570-577.
[172] Kang T., Kimura I., Shimizu Y. Responses of bed morphology to vegetation growth and flood discharge at a sharp river bend [J]. *Water*, 2018, 10(2): 223.
[173] Yang S., Bai Y., Xu H. Experimental analysis of river evolution with riparian vegetation [J]. *Water*, 2018, 10(11): 1500.
[174] Zen S., Perona P. Biomorphodynamics of river banks in vegetated channels with self-formed width [J]. *Advances in Water Resources*, 2020, 135: 103488.
[175] Andrews E. D. Bed-material entrainment and hydraulic geometry of gravel-bed rivers in Colorado [J]. *Geological Society America Bulletin*, 1984, 95: 371-378.
[176] Hey R. D., Thorne C. R. Stable channels with mobile gravel beds [J]. *Journal of Hydraulic Engineering, ASCE*, 1986, 112(8): 671-689.
[177] Huang H. Q., Nanson G. C. Vegetation and channel variation; a case study of four small streams in southeastern Australia [J]. *Geomorphology*, 1997, 18(3-4): 237-249.
[178] Ikeda S., Izumi N. Width and depth of self-formed straight gravel rivers with bank vegetation [J]. *Water Resources Research*, 1990, 26(10): 2353-2364.
[179] Bertoldi W., Gurnell A. M., Drake N. A. The topographic signature of vegetation development along a braided river: Results of a combined analysis of airborne lidar, color air photographs, and ground measurements [J]. *Water Resources Research*, 2011, 47(6): 1-13.
[180] Jang C. L., Shimizu Y. Vegetation effects on the morphological behavior of alluvial channels [J]. *Journal of Hydraulic Research*, 2007,4 5(6): 763-772.
[181] Kujanová K., Matoušková M., Hošek Z. The relationship between river types and land cover in riparian zones [J]. *Limnologica*, 2018, 71: 29-43.
[182] Mackin J. H. Cause of braiding by a graded river [J]. *Geological Society of America Bulletin*, 1956, 67(12): 1717-1718.
[183] Gurnell A. M., Bertoldi W., Corenblit D. Changing river channels: The roles of hydrological processes, plants and pioneer fluvial landforms in humid temperate, mixed load, gravel bed rivers [J]. *Earth-Science Reviews*, 2012, 111(1-2): 129-141.
[184] Page K., Frazier P., Pietsch T. et al. Channel change

following European settlement: Gilmore Creek, southeastern Australia [J]. *Earth Surface Processes and Landforms*, 2007, 32(9): 1398-1411.
[185] Naiman R. J., Decamps H., McClain M. E. Riparia [M]. Rotterdam, The Netherlands: Elsevier, 2005.
[186] Mahoney J. M., Rood S. B. Streamflow requirements for cottonwood seedling recruitment-An integrative model [J]. *Wetlands*, 1998, 18(4): 634-645.
[187] Amlin N. A., Rood S. B. Inundation tolerances of riparian willows and cottonwoods [J]. *Journal of the American Water Resources Association*, 2001, 37(6): 1709-1720.
[188] Amlin N. M., Rood S. B. Comparative tolerances of riparian willows and cottonwoods to water-table decline [J]. *Wetlands*, 2002, 22(2): 338-346.
[189] Bhattacharjee J., Taylor Jr J. P., Smith L. M. et al. The importance of soil characteristics in determining survival of first-year cottonwood seedlings in altered riparian habitats [J]. *Restoration Ecology*, 2008, 16(4): 563-571.
[190] Braatne J. H., Jamieson R., Gill K. M. et al. Instream flows and the decline of riparian cottonwoods along the Yakima River, Washington, USA [J]. *River Research and Applications*, 2007, 23(3): 247-267.
[191] Dixon M. D., Turner M. G. Simulated recruitment of riparian trees and shrubs under natural and regulated flow regimes on the Wisconsin River, USA [J]. *River Research and Applications*, 2006, 22(10): 1057-1083.
[192] Greet J., Webb J A., Cousens R. D. The importance of seasonal flow timing for riparian vegetation dynamics: A systematic review using causal criteria analysis [J]. *Freshwater Biology*, 2011, 56(7): 1231-1247.
[193] Bradley C. E., Smith D. G. Plains cottonwood recruitment and survival on a prairie meandering river floodplain, Milk River, southern Alberta and northern Montana [J]. *Canadian Journal of Botany*, 1986, 64(7): 1433-1442.
[194] Moggridge H. L., Gurnell A. M. Controls on the sexual and asexual regeneration of Salicaceae along a highly dynamic, braided river system [J]. *Aquatic Sciences*, 2009, 71(3): 305-317.
[195] Solari L., van Oorschot M., Belletti B. et al. Advances on modelling riparian vegetation-hydromorphology interactions [J]. *River Research and Applications*, 2016, 32(2): 164-178.
[196] Benjankar R., Egger G., Jorde K. et al. Dynamic floodplain vegetation model development for the Kootenai River, USA [J]. *Journal of Environmental Management*, 2011, 92(12): 3058-3070.
[197] Coulthard T. J., Hicks D. M., Van De Wiel M. J. Cellular modelling of river catchments and reaches: Advantages, limitations and prospects [J]. *Geomorphology*, 2007, 90(3-4): 192-207.
[198] Hooke J. M., Brookes C. J., Duane W. et al. A simulation model of morphological, vegetation and sediment changes in ephemeral streams [J]. *Earth Surface Processes and Landforms*, 2005, 30(7): 845-866.
[199] Camporeale C., Perona P., Porporato A. et al. Hierarchy of models for meandering rivers and related morphodynamic processes [J]. *Reviews of Geophysics*, 2007, 45: 446-447.
[200] Imran J., Parker G., Pirmez C. A nonlinear model of flow in meandering submarine and subaerial channels [J]. *Journal of Fluid Mechanics*, 1999, 400: 295-331.
[201] Zolezzi G., Seminara G. Downstream and upstream influence in river meandering. Part 1. General theory and application to overdeepening [J]. *Journal of Fluid Mechanics*, 2001, 438: 183-211.
[202] Seminara G., Zolezzi G., Tubino M. et al. Downstream and upstream influence in river meandering. Part 2. Planimetric development [J]. *Journal of Fluid Mechanics*, 2001, 438: 213-230.
[203] Van De Wiel M. J., Darby S. E., Bennett S. A. S. Numerical modeling of bed topography and bank erosion along tree-lined meandering rivers: Riparian vegetation and fluvial geomorphology [M]. Washington, DC, USA: American Geophysical Union, 2004, 267-282.
[204] Baptist M. J., van den Bosch L. V., Dijkstra J. T. et al. Modelling the effects of vegetation on flow and morphology in rivers [J]. *Large Rivers*, 2003, 15(1-4): 339-357.
[205] Baptist M. J., Penning W. E., Duel H. et al. Assessment of the effects of cyclic floodplain rejuvenation on flood levels and biodiversity along the Rhine river [J]. *River Research and Applications*, 2004, 20(3): 285-297.
[206] Crosato A., Saleh M. S. Numerical study on the effects of floodplain vegetation on river planform style [J]. *Earth Surface Processes and Landforms*, 2011, 36(6): 711-720.
[207] Perucca E., Camporeale C., Ridolfi L. Influence of river meandering dynamics on riparian vegetation pattern formation [J]. *Journal of Geophysical Research: Biogeosciences*, 2006,111(G1): G01001.
[208] Perucca E., Camporeale C., Ridolfi L. Significance of the riparian vegetation dynamics on meandering river morphodynamics [J]. *Water Resources Research*, 2007, 43(3): W03430.
[209] Camporeale C., Ridolfi L. Interplay among river meandering, discharge stochasticity and riparian vegetation [J]. *Journal of Hydrology*, 2010, 382(1-4): 138-144.
[210] Muneepeerakul R., Rinaldo A., Rodriguez-Iturbe I. Effects of river flow scaling properties on riparian width and vegetation biomass [J]. *Water Resources Researc*h, 2007, 43(12): W12406.
[211] Perona P., Molnar P., Savina M. et al. An observation-based stochastic model for sediment and vegetation dynamics in the floodplain of an Alpine braided river [J]. *Water Resources Research*, 2009, 45(9): W09418.
[212] Poggi D., Katul G. G. Turbulent flows on forested hilly terrain: The recirculation region [J]. *Quarterly Journal of the Royal Meteorological Society*, 2007, 133(625): 1027-1039.
[213] Poggi D., Katul G. G. An experimental investigation of the mean momentum budget inside dense canopies on narrow gentle hilly terrain [J]. *Agricultural and Forest Meteorology*, 2007, 144(1-2): 1-13.
[214] Poggi D., Katul G. G., Finnigan J. J. et al. Analytical models for the mean flow inside dense canopies on gentle hilly terrain [J]. *Quarterly Journal of the Royal Meteorological Society*, 2008, 134(634): 1095-1112.
[215] Poggi D., Katul G. G., Albertson J. D. et al. An experimental investigation of turbulent flows over a hilly surface [J]. *Physics of Fluids*, 2007, 19(3): 36601.
[216] Poggi D., Katul G. The ejection-sweep cycle over bare and forested gentle hills: A laboratory experiment [J]. *Boundary-Layer Meteorology*, 2007, 122(3): 493-515.
[217] Katul G. G., Poggi D. The effects of gentle topographic variation on dispersal kernels of inertial particles [J]. *Geophysical Research Letters*, 2012, 39(3): L03401.
[218] Beven K. A manifesto for the equifinality thesis [J]. *Journal of Hydrology*, 2006, 320(1-2): 18-36.
[219] Julien P. Y. Erosion and sedimentation [M]. Cambridge, UK: Cambridge University Press, 1995.